論文 / 著書情報
Article / Book Information

題目(和文)	
Title(English)	The Effect of 5-Aminolevulinic Acid and Sodium Ferrous Citrate on Mitochondrial Properties in Myoblast and Cancer Cells
著者(和文)	SuprihadiArif
Author(English)	Arif Suprihadi
出典(和文)	学位:博士(工学), 学位授与機関:東京工業大学, 報告番号:甲第12213号, 授与年月日:2022年9月22日, 学位の種別:課程博士, 審査員:小倉 俊一郎,山本 直之,小畠 英理,三重 正和,白木 伸明
Citation(English)	Degree:Doctor (Engineering), Conferring organization: Tokyo Institute of Technology, Report number:甲第12213号, Conferred date:2022/9/22, Degree Type:Course doctor, Examiner:,,,,
学位種別(和文)	博士論文
Type(English)	Doctoral Thesis

Year 2022

Doctoral thesis

The Effect of 5-Aminolevulinic Acid and Sodium Ferrous Citrate on Mitochondrial Properties in Myoblast and Cancer Cells

Tokyo Institute of Technology

School of Life Science and Technology

Life Science and Technology Major

in

Life Science and Technology Course

Arif Suprihadi

Academic Supervisor

Assoc. Prof. Dr. Shun-Ichiro Ogura

TABLE OF CONTENTS

LIST OF ABBREVIATIONS

LIST OF ABBREVIATIONS

%	Percentage
°C	Celcius
ABAM	Antibiotic antimycotic
ADP	Adenosine diphosphate
ALA	5-Aminolevulinic acid
ALAS	δ-aminolaevulinic synthase
ANOVA	Analysis of variance
ATP	Adenosine triphosphate
CO_2	Carbon dioxide
COX	Cytochrome *c* oxidase
DCF	2',7'-dichlorodihydrofluorescein
DCFH-DA	2',7'-dichlorodihydrofluorescin diacetate
DMEM	Dulbecco's modified eagle medium
DTT	Dithiothreitol
ETC	Electron transport chain
FBS	Fetal bovine serum
Fe-S	Iron-sulfur
FECH	Ferrochelatase
GM	Growth medium
HBSS	Hank's balanced salt solution
HO-1	Heme oxygenase-1
HPLC	High performance Liquid Chromatography
HRP	Horseradish peroxidase
HS	Horse serum
mg	Miligram
mL	Milliliter
mM	Milimolar
mM	Millimolar
mRNA	Messenger RNA
mt-DNA	Mitochondrial DNA
MTT	3-[4,5-dimethylthiazol-2-yl]-2,5-diphenyl tetrazolium bromide
NaCl	Sodium chloride

NaOH	Sodium hydoxide
nM	Nanomolar
nm	Nanometer
O_2	Oxygen
OXPHOS	Oxidative phosphorylation
PBS	Phosphate buffer saline
PDD	Photodynamic diagnosis
PDT	Photodynamic therapy
PEPT	Peptide transporter
PpIX	Protoporphyrin IX
qRT-PCR	Quantitative real-time polymerase chain reaction
Redox	Reduction-oxidation
RFU	Relative fluorescence units
ROS	Reactive oxygen species
RPMI	Roswell park memorial institute medium
SD	Standard deviation
SDS-PAGE	Sodium dodecyl sulfate–polyacrylamide gel electrophoresis
SFC	Sodium ferrous citrate
TBST	Tris-buffered saline with 0.05 % (v/v) Tween 20
µL	Microliter
µM	Micromolar
µmol	Micromole

CHAPTER 1
INTRODUCTION

1.1 ROLE OF MITOCHONDRIA IN ANIMAL CELLS

1.1.1 Overview of mitochondria

The originated of mitochondria was believed from the engulfment of an α-proteobacterium by a precursor of the modern eukaryotic cell (Lane & Martin, 2010). Mitochondria are organelles that have double layer membrane-bound cytoplasmic present in most eukaryotic cells, each of their membranes have different functions. Mitochondria are relatively small organelle, mostly from 0.75 to 3 micrometers and only visible when they are stained. Mitochondria can be divided into different compartments or regions depicted in **Figure 1.1**, and each of them has their own special functions and distinct roles as tabulated in **Table 1.1** (Shimizu, 2019). Basically, mitochondria have five major regions namely: Outer membrane, small molecules can pass freely through this outer membrane; intermembrane space, the region between the double layer membranes; inner membrane, proteins are held by this membrane; cristae, these are the folds of the inner membrane; and matrix, the space within inner membrane and the location of mt-DNA.

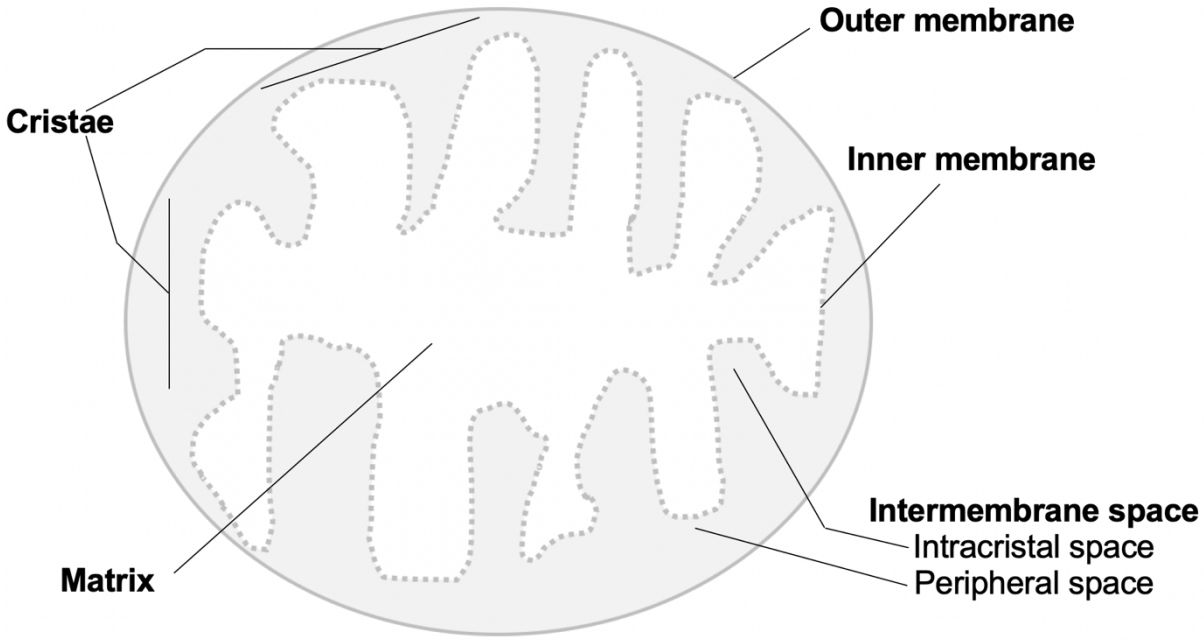

Figure 1.1 Simplified structure of a mitochondria

Mitochondria have been recognized as the center of metabolic (Nunnari, 2008), carried out various metabolic functions, such as the urea cycle (Smith & Garg, 2017) and gluconeogenesis (Stark *et. al.,* 2014). At the same time, they are controlling/signalling calcium (Ca^{2+}) which is essential for maintaining homeostasis of

eukaryotic cells (Schatz, 1995), as it involved in reactive oxygen species (ROS) production, synthesis of apo lipids, heme and steroids, and the induction of apoptosis (Wallace, 1999; Stöckl *et. al.,* 2006). However, they well are known as the organelle that producing energy in cells. Almost all of the energy in cell or adenosine triphosphate (ATP) is synthesized during the metabolism of glucose in mitochondria and it carried out through the oxidative phosphorylation system (Bertram *et. al.,* 2006).

Table 1.1 Functions of various regions of the mitochondria

Typical function	Key molecules
Protein transport (outer membrane)	Tom complex
Adenine nucleotide balance (intermembrane space)	Adenylate kinase
Oxidative phosphorylation (inner membrane)	Electron transfer complexes
Metabolism & mtDNA replication (matrix)	Enzyme of TCA cycle, urea cycle, β-oxidation, gluconeogenesis, and mtDNA

1.1.2 Oxidative phosphorylation system

In the previous sub-chapter, it was explained that each region in mitochondria has different and its own specific functions. The inner membrane of mitochondria is the energy source of mitochondria, this membrane transposes energy through the oxidative phosphorylation (OXPHOS) system, the main process that responsible of the energy production in eukaryotic cells by producing ATP, the basic unit of energy for metabolic processes (Saraste, 1999). ATP is produced using a proton gradient across the inner membrane. Mitchell proposed his chemiosmotic theory which states about the entire general sequence of biochemical events leading to ATP synthesis (Mitchell, 1966).

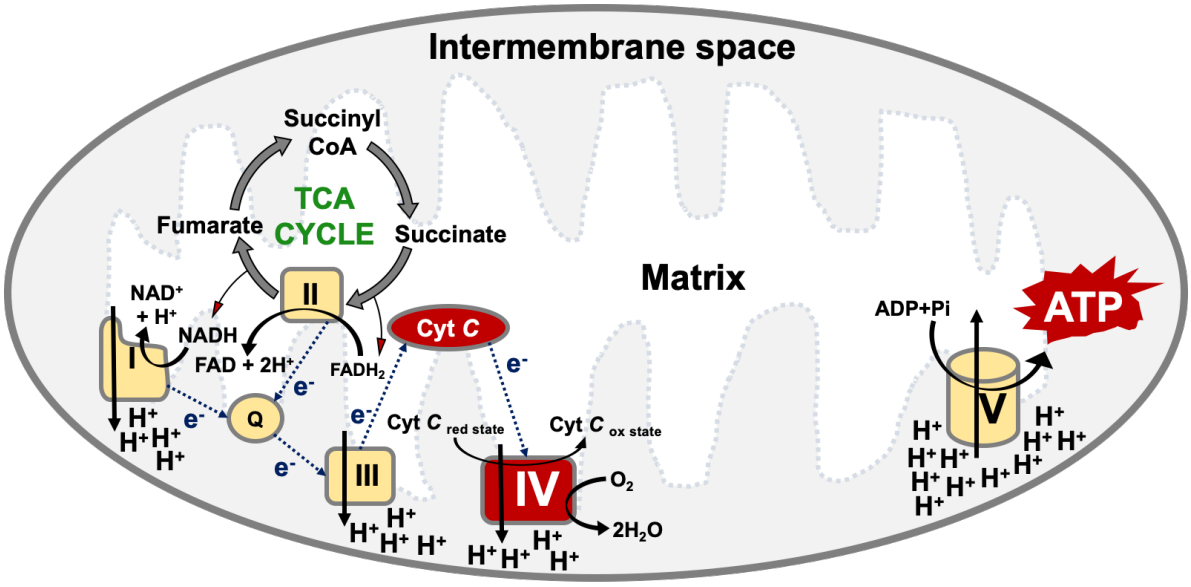

Figure 1.2 Five major membrane complexes in the electron transport chain involved in oxidative phosphorylation system

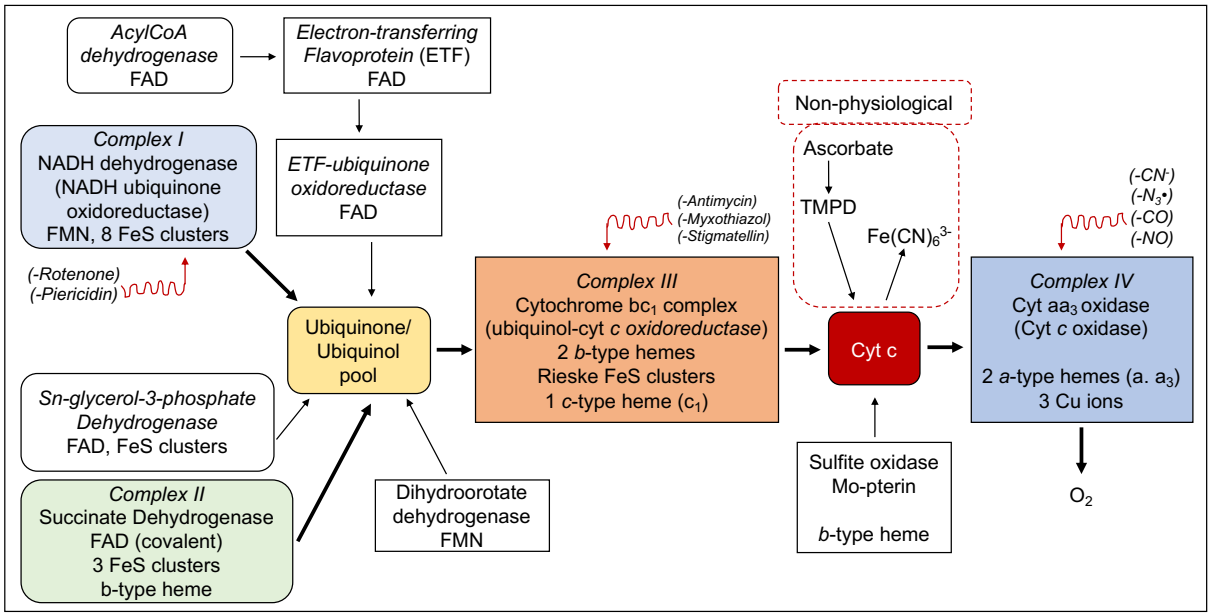

Figure 1.3 Overview of the redox carriers in the mitochondrial respiratory chain and their relation to the four respiratory chain complexes

ATP production in the inner membrane of mitochondria is carried out through the oxidative phosphorylation system (**Figure 1.2**). It comprised of a series of five major membrane complexes namely NADH dehydrogenase (complex I); succinate dehydrogenase (complex II); cytochrome *c* reductase (complex III); cytochrome *c*; cytochrome *c* oxidase; COX (complex IV); and ATP synthase (complex V), it called electron transport chain (ETC) (**Figure 1.3**) (Palmeira & Ramalho-Santos, 2011;

Hüttemann *et. al.,* 2008). Each complex in ETC has their own function as tabulated in **Table 1.2**. The electron transport chain uses the electrons from electron carriers to create a chemical gradient that can be used to power oxidative phosphorylation. The electron transport chain transfers electrons through the reduction-oxidation (redox) potential span of complex I until complex IV, from NAD^+/NADH couple to the $O_2/2H_2O$ couple.

Table 1.2 Functions of electron transport chain complexes

Protein	Role	Citations
Complex I	Passage of two electrons from NADH to ubiquinone, and pumps four protons across the membrane	Sazanov & Hinchliffe (2006)
Complex II	Passage of two electrons from $FADH_2$ to ubiquinone	Maklashina & Cecchini (2010)
Ubiquinone/ ubiquinol	Receives electrons from complex I and complex II, once ubiquinone is reduced to ubiquinol, it delivers its electron to complex III	Maklashina & Cecchini (2010)
Complex III	Pumps protons across the membrane and passes its electron to cytochrome *c*	Crofts (2004)
Cytochrome *c*	Accept electron from complex III and donates it to complex IV	Lange and Hunte (2002)
Complex IV	Pumps protons and transfer of 4 electrons from the reduced cytochrome *c* to oxygen to produce water	Hyung *et. al.,* (2012)
Complex V	Tiny generator turned by the force of protons to produce ATP	Muench *et al.,* (2011)

1.1.3 Relationship between mitochondrial disorders and cytochrome *c* oxidase deficiency

Mitochondria have long been recognized as an essential role for various biological process in cells, including in the lifespan of cells (Hwang *et. al.,* 2012). Moreover, the functions of mitochondria are the main factor of organism longevity. One of the main targets of xenobiotic-induced bioenergetics failure is mitochondria (Wallace & Starkov, 2000; Palmeira & Rolo, 2004). Mitochondrial abnormalities are strongly involved in the onset and progression of aging and diseases as shown in **Figure 1.4**. Dysfunction in mitochondria were notoriously is a key player in a variety of human disorders (Ghezzi & Zeviani, 2018), such as aging, diabetes, cancer, and neurodegenerative diseases including Parkinson's, Huntington's and Alzheimer diseases (Allen *et. al.,* 2018; Gris, 2009; Gris, 2013). Absolutely, dysfunction of mitochondria disrupts the ATP synthesis process (Lebiedzinska *et. al.*, 2013). Therefore, the dysfunction of mitochondria can lead to cell death by depletion of ATP and calcium dysregulation (Di Lisa & Bernardi, 1998).

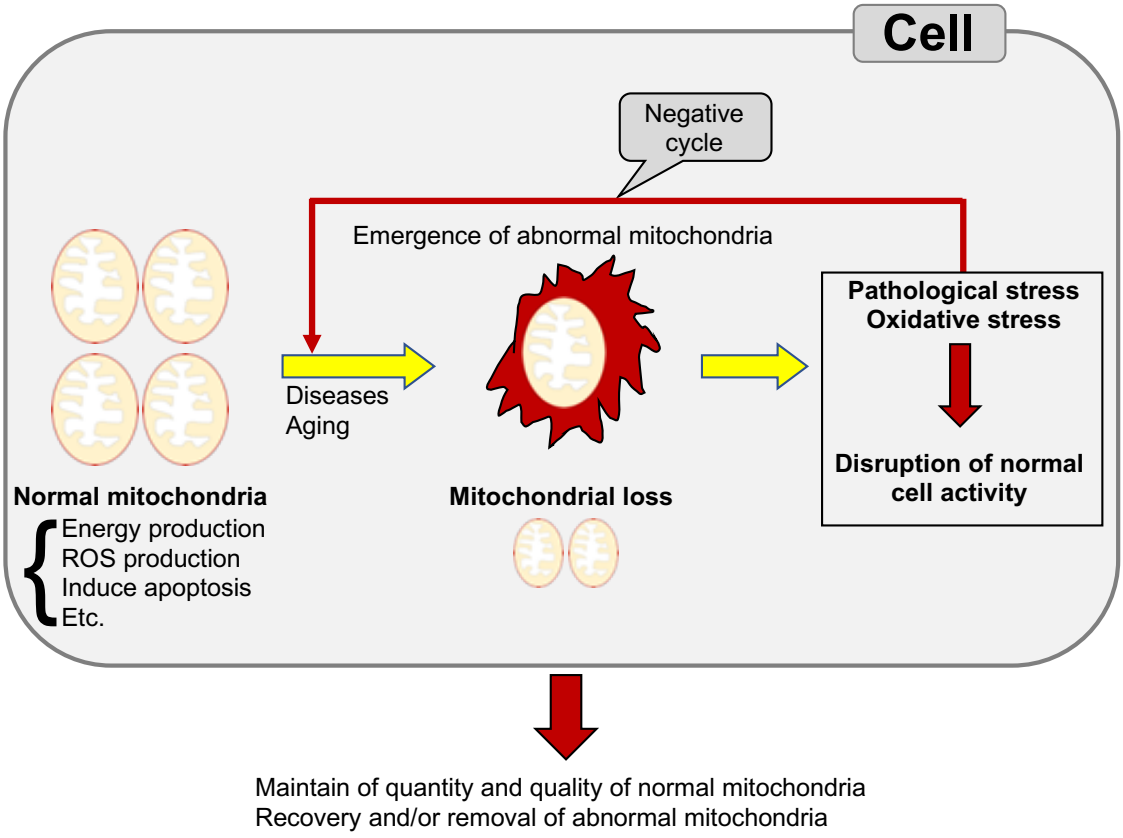

Figure 1.4 Relationship between the conditions of mitochondria and the progressing of aging and diseases

One of the frequent factors that cause of mitochondrial dysfunction is the deficiency of COX and it is associated with a wide spectrum of clinical phenotype (Willis *et. al.,* 2009; Coenen. *et. al.,* 1999). COX is the last enzyme in the electron transport chain and it is a regulation site for mitochondrial OXPHOS system. COX is responsible for catalyzes the transfer of electrons from reduced cytochrome *c* to molecular oxygen (Wilson & Brunori, 1995; Calhoun *et.al,* 1994). In addition, it also reported that changes of COX function were suggested in a wide array of some disease conditions such as neurodegenerative diseases, including Alzheimer's and Parkinson's diseases, and age-related loss of COX activity (Paradies *et. al.,* 1993; Sohal, 1993). In the previous experiment, it was reported that COX activities were lower in tumors cells compared to normal cells, it can be categorized as defects in the oxidative phosphorylation (Sugiyama *et. al.,* 2012; Sugiyama *et. al.,* 2013). Therefore, an approach aimed at alleviating the symptoms of mitochondrial dysfunction is needed to be carried out. Moreover, the actions to preserve the mitochondrial activity and to prevent the inactivation of COX are very important.

1.2 METABOLIC AND BIOACTIVITY EFFECTS OF 5-AMINOLEVULINIC ACID AND SODIUM FERROUS CITRATE

1.2.1 Metabolic mechanism of 5-aminolevulinic acid

5-aminolevulinic acid (ALA) (**Figure 1.5**) is a type of non-toxic compound and this amino acid is naturally synthesized in vivo in plants and animals (Layer *et. al.,* 2010). ALA is known to be the first compound in the porphyrin biosynthesis pathway, the pathways that lead to heme and ALA acts as vital cofactors in vivo. In particular, porphyrins that bind to a metal ion called metalloporphyrins are essential and have diverse functions and acts as cofactors indispensable for the activity of various functional proteins. For instance, porphyrins that bind to an iron ion is heme, an essential oxygen-carrying component of functional hemoglobin in red blood cells and myoglobin in muscle cells. Therefore, the biosynthesis pathway of ALA is an important mechanism for life.

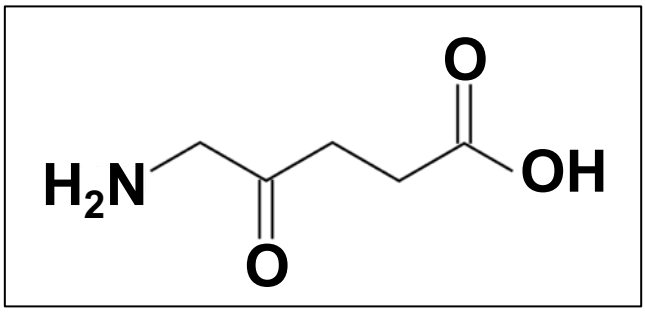

Figure 1.5 Molecular structure of ALA

1.2.2 Bioactivity effects of ALA

In the previous study it was mentioned that δ-aminolaevulinic synthase (ALAS), is the rate-limiting enzyme in porphyrin biosynthesis pathway in mitochondria (Woodard & Dailey, 2000). Therefore, the addition of ALA exogenously can be expected to increase the number of metalloporphyrins. Since it acts as cofactors indispensable for the activity of various functional proteins, promotion of biosynthesis of metalloporphyrins such as heme is thought to affect the expression and activity of various protein especially hemeprotein. Furthermore, it was reported that in plants the addition of ALA increases the chlorophyll precursor Mg-porphyrin, which brings promoting effect. In the previous experiments in our laboratory also revealed that the addition of ALA to the cells increases heme precursor protoporphyrin IX (PpIX). Moreover, it is already clearly shown that the expression and activity of various hemoproteins such as COX are likely to increase with the addition of ALA (Sugiyama *et. al.,* 2014; Ogura *et. al.,* 2011; Miura *et. al.,* 2015). In addition, ALA has been widely used in research on photosensitizers in the medical field. For example, in photodynamic therapy (ALA-PDT) and photodynamic diagnosis (ALA-PDD) because ALA induces the accumulation of porphyrin in the specific cancer tissues (Stummer *et. al.,* 2006; Krammer & Plaetzer, 2008). As mentioned above, ALA has various physiologically active functions and, in the future, further applications of ALA as a physiologically active substance are expected to be developed.

1.2.3 The properties sodium ferrous citrate

Sodium Ferrous Citrate (SFC) as shown in **Figure 1.6** is an iron provider. It is odorless and greenish white powder, and soluble chelated iron (non-ionic iron). It contains 10.0 to 11.0% iron. It is synthesized from ferrous sulfate and sodium citrate. Because it is an iron provider it can help to increase the iron levels in the cell. Moreover,

it can be widely used as a food additive and supplement ingredient (Yamashita *et. al.,* 2014; Komatsu *et. al.,* 2021).

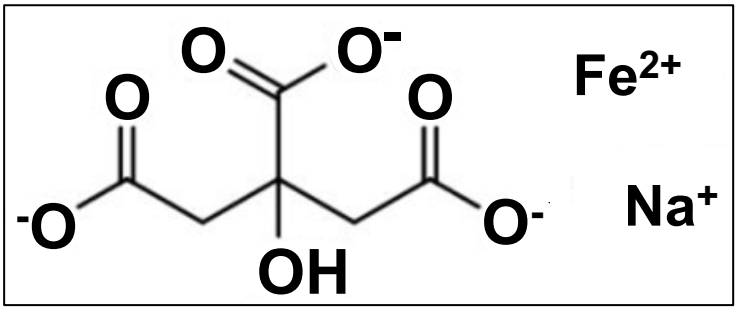

Figure 1.6 Molecular structure of SFC

1.2.4 The relationship between ALA, SFC, and heme proteins

Heme is protophorphyrin that binds to iron and is essential oxygen carrying component of functional hemoglobin in red cells and myoglobin in muscle cells. A heme is an organic compound, ring shaped molecule. Because of its special structure, a heme is capable of holding or hosting an iron molecule. Heme has diverse biological functions including electron transfer in electron transport chain (ETC) (Reedy, C. J., & Gibney, B. R. 2004). The biosynthesis of heme in vivo is shown in **Figure 1.7**. In animals, heme is synthesized in mitochondria. Where the pathway is initiated by the synthesis of ALA from glycine and succinyl CoA in mitochondria which is activated by the rate-limiting enzyme δ-aminolaevulinic synthase (ALAS), then ALA is once transported to the cytoplasm. On the other hand, when ALA was added exogenously in cells, it is taken to cytoplasm by the peptide transporter namely PEPT1 and PEPT2. After that, through the porphyrin pathway, ALA as heme precursor is converted to protoporphyrin IX. Heme is generated by the insertion of ferrous ion into protoporphyrin IX. Exogenously administered ALA and SFC are absorbed into the cytoplasm, and then used as a substrate for protoporphyrin IX and source of free iron ion to form heme. Heme is degraded to carbon monoxide (CO), iron, and biliverdin by haem oxygenase-1 (HO-1) (Shimura *et. al.,* 2019).

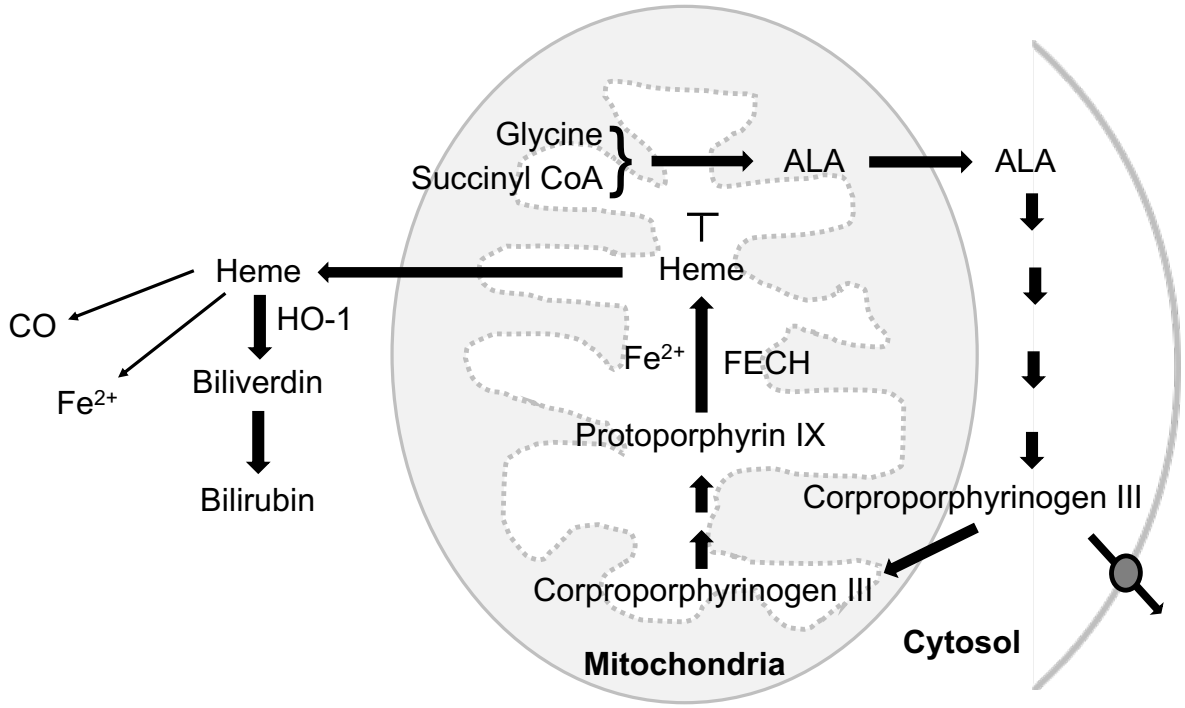

Figure 1.7 Diagram showing the heme biosynthesis pathway and how exogenous ALA is involved

Furthermore, Mitochondrial respiratory chain complexes III, IV and cytochrome *c* contain heme (Paoli *et. al.,* 2002), which is generated by the insertion of Fe2+ into protoporphyrin IX. ALA combined with SFC was reported to enhance heme production, leading to respiratory complex and heme oxygenase-1 (HO-1) upregulation (Wang *et. al.,* 2017). Moreover, the increasing of heme production by the addition of ALA, SFC, and combined ALA+SFC has the possibility to increase the protein expression level of heme proteins in mitochondria as illustrated in **Figure 1.8**. Taken together, it is assumed that the effect of ALA, SFC, and combined ALA+SFC treatment can improves mitochondrial respiratory chain functions, leading to an enhances cytochrome *c* oxidase (COX) activity and also increase in oxidative phosphorylation (OXPHOS), and ATP production.

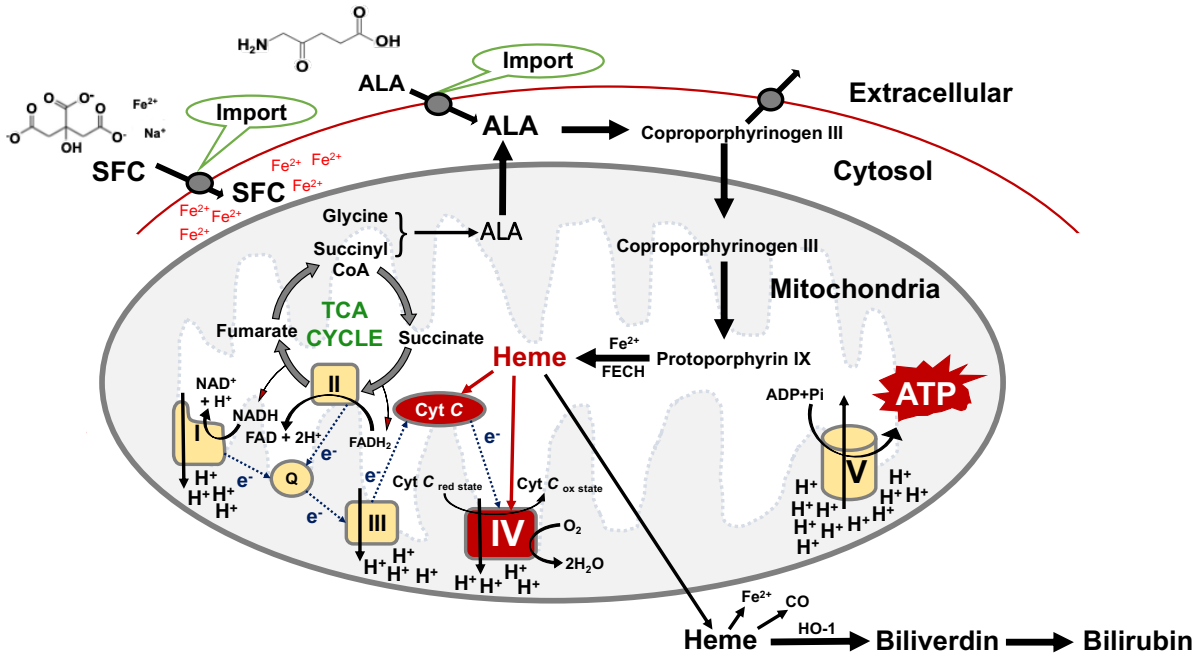

Figure 1.8 Schematic illustration of the relationship between heme biosynthesis pathway and electron transport chain

1.3 AIMS & OBJECTIVES OF THIS STUDY

The main aim of this research is to study the effects of the addition ALA, SFC, and ALA+SFC to the cells on the oxidative phosphorylation system and mitochondrial activities. This study also trying to improve the mitochondrial activity and prevent the inactivation of COX by the addition of ALA, SFC, and ALA+SFC in myoblast cells. Myoblast cell is an ideal cell line to study about mitochondria functions because of myotubes are muscle fibers that need a lot of energy (ATP) and rely on OXPHOS system. In addition, it is an attractive tissue because of the minimally invasive character of sampling and the amount of cell material obtained by culturing. Furthermore, for studying the effect of ALA, SFC, and ALA+SFC on cancer cells, a human gastric cancer cell namely MKN45 cells were also used in this experiment. In cancer cells, the study focused on the effect of ALA during photodynamic therapy (PDT). In addition, in the previous study, SFC is reported to increase COX activity. So, this study also aims to improve the COX activity by the addition of SFC that can promote reactive oxygen species (ROS) generation, which has a cytotoxic effect that can kill the cancer cell.

CHAPTER 2
5-AMINOLEVULINIC ACID IMPROVED MITOCHONDRIAL ACTIVITIES BY STIMULATE OXPHOS SYSTEM INDEPENDENT OF MITOCHONDRIAL CONTENT AND BIOGENESIS IN MYOBLAST CELLS

2.1 INTRODUCTION

It is believed that the number and function of mitochondria decrease (dysfunction of mitochondria) during the aging process and disease and resulting decrease in energy production and increase mitochondria or oxidative stress that lead further development of aging and disease (Desler *et. al.,* 2011; Bonawitz *et. al.,* 2007; Gris, 2013; Moghaddas *et. al.,* 2003). Therefore, it is really important to maintain the function of mitochondria including the mitochondrial content and mitochondrial biogenesis. Previous experiments revealed that heme precursor ALA improves the heme biosynthesis. Moreover, it also demonstrated that ALA administration both *in vitro and in vivo* increases mitochondrial function including increased in cytochrome *c* oxidase protein expression levels (Sugiyama, 2011). However, the effect of ALA towards overall electron transport chain, mitochondrial content, and mitochondrial biogenesis remains unclear. Therefore, in this chapter, we focused on those concerns in myoblast cell as illustrated in **Figure 2.1**.

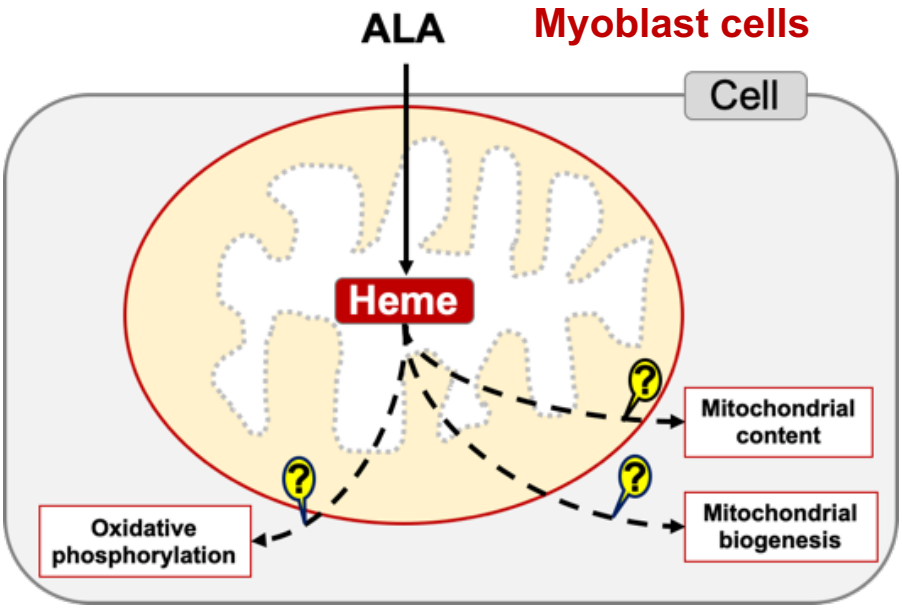

Figure 2.1 Conceptual diagram of addition of exogenous ALA

2.2 MATERIALS AND METHODS

Chemicals

DMEM-high glucose medium, DMEM-low glucose medium, and antibiotic-antimitotic mixed stock medium (ABAM) were purchased from Nacalai Tesque (Kyoto, Japan). Fetal bovine serum (FBS) and horse serum (HS) were purchased from

Invitrogen (Carlsbad, California, USA). Aminolevulinic acid (ALA) was purchased from Cosmo Bio Co. Ltd. (Tokyo, Japan).

Cell culture

Mouse myoblast cells, namely the C2C12 cell line, were obtained from RIKEN, Japan. Myoblast cells were cultured in DMEM-high glucose culture medium. Cells were incubated and followed by addition of 10% FBS and 10% ABAM, at 37°C in a 5% CO_2 incubator. When cells were reached 70% – 80% confluency previous medium was replaced with DMEM-low glucose culture medium (differentiation medium) followed by addition of 2% HS and 10% ABAM. Differentiation medium was replaced with fresh ones every 48 hours for 6 days. Cell number for seeding in various experiments is tabulated in **Table 2.1**.

Table 2.1 Amount of cell seeded for each experiment

Experiments	Seeding cell number (cells / well)
Heme production level	0.5×10^6 cells
Protein expression level of electron transport chain	
mt-DNA expression level	
Mitochondrial content analysis	
mRNA expression level of mitochondrial biogenesis related gene	
COX activity measurement	0.5×10^7 cells
ATP production level quantification	

Heme production quantification using High performance Liquid Chromatography (HPLC)

Cells were seeded in 35 mm dishes and incubated at 37°C in a 5% CO_2 incubator to reach confluency then differentiated to be myotube. Experiments were carried out in triplicates per sample. Addition of ALA was carried out and cells were further incubated under the same condition for the next 96 hours. In order to quantify extracellular heme, medium with serum should be avoided but not if only quantify intracellular heme. Cells on 35 mm dishes first were placed on ice and washed with

cold PBS 3 times. Cells were lysed with 150 µL 0.1 N NaOH. a volume of 50 µL of cell suspension from each sample were taken out and added into a new 1.5 mL centrifuge tube containing 150 µL of (1 : 9; 1 M CH_3COONH_3, 12.5% acetonitrile, pH 5.2 : 50 mM CH_3COONH_3, 80% acetonitrile, pH 5.2). Cells suspension then underwent centrifugation under 10,000 x *g* for 10 minutes. Supernatants were recovered and pellets were discarded.

HPLC analysis of heme was carried out using Type Prominence System (Shimadzu Manufacturing Co., Kyoto, Japan) equipped with reverse phase C18 column (CAPCELL PAK, C18, SG300, 5 µm, 4.6 mm x 250 mm, Osaka Soda Co. Ltd., Osaka) while maintaining at temperature of 40°C. Mobile phase A, comprising 1 M ammonium acetate solution containing 12.5% acetonitrile (adjusted to pH 5.2), and mobile phase B made up of 50 mM ammonium acetate solution containing 80% acetonitrile, were used in elution of heme. 50% mobile phase B was first directed at a flow rate of 1.0 mL / min for 10 minutes following by driving mobile phase B into column from a linear gradient ranging from 90% for 10 minutes and finally 90% mobile phase B at a flow rate 2.0 mL / min for another 10 minutes elution program. Protein concentration of each samples were determined using Bradford's method using Quickstart Bradford 1 x Dye reagent (Biorad laboratories, Inc., Hercules, California, USA).

Real-time polymerase chain reaction (PCR)

Total RNA extractions from culture cells were carried out using RNA extraction kit NucleoSpin® RNA II (MACHERY-NAGEL, Düren, Mannheim, Germany). Extracted RNA were transcript into 1 µg single stranded cDNA via a reverse transcription reaction using PrimeScript RT reagent Kit with gDNA Eraser (TaKaRa Bio, Shiga, Japan). The expression levels of TFAM, NRF-1, NRF-2, PGC-1α, and actin (housekeeping gene / internal control) were then quantified using Thermal Cycler Dice® Real Time System Single (TaKaRa Bio, Shiga, Japan). The primers used in amplification were tabulated in **Table 2.2**. Primers set specific to each gene were used in quantitative reverse transcription polymerase chain reaction (qRT-PCR). Expression level of each targeted gene were then standardized by dividing with the expression level of actin which used an internal control.

Table 2.2 Primers sequences used in gene amplification

Gene	Sense / Antisense	Sequence
TFAM	Sense	5'-GCAAAGGATGATTCGGCTCAGGGAA-3'
	Antisense	3'-CCGGATCGTTTCACACTTCGACGG-5'
NRF-1	Sense	5'-GGTGTTTGGCGCAGCACCTT-3'
	Antisense	3'-CTCTGGGATAAATGCCCGAAGCT-5'
NRF2	Sense	5'-CAAGACTTGGGCCACTTAAAAGAC-3'
	Antisense	3'-AGTAAGGCTTTCCATCCTCATCAC-5'
PGC- 1α	Sense	5'-AAGACGATTGCCCTCATTT-3'
	Antisense	3'-AGTGCTAAGACCGCTGCATT-5'
Actin	Sense	5'-TGAGAGGGAAATCGTGCGTG-3'
	Antisense	3'-TGCTTGCTGATCCACATCTGC-5'

Total mitochondrial DNA (mtDNA) from culture cells were carried out using DNA extraction kit NucleoSpin® RNA II (MACHERY-NAGEL, Düren, Mannheim, Germany). The expression levels of mt-COX1, mt-COX2, mt-ND1 and actin (housekeeping gene / internal control) were then quantified using Thermal Cycler Dice® Real Time System Single (TaKaRa Bio, Shiga, Japan). The primers used in amplification were tabulated in **Table 2.3**. Primers set specific to each gene were used in real-time PCR. Expression level of each targeted gene were then standardized by dividing with the expression level of actin which used an internal control.

Table 2.3 Primers sequences used in gene amplification

Gene	Sense / Antisense	Sequence
mt-COX1	Sense	5'-ACTATACTACTAACAGACCG-3'
	Antisense	3'-GGTTCTTTTTTTCCGGAGTA-5'
mt-COX2	Sense	5'-AACCATAGGGCACCAATGATAC-3'
	Antisense	3'-GGATGGCATCAGTTTTAAGTCC-5'
Mt-ND1	Sense	5'-GTTGGTCCATACGCATTTT-3'
	Antisense	3'-TGGGTGTGGTATTGGTAGGG-5'
Actin	Sense	5'-TGAGAGGGAAATCGTGCGTG-3'
	Antisense	3'-TGCTTGCTGATCCACATCTGC-5'

Western blotting

Western blotting experiments were carried out to quantify the expression level of proteins in cell using modified method based on Kogot-Levin *et. al.,* (2016). Cells were first washed with PBS (-), followed by addition lysis buffer A [50 mM Tris-HCl (pH 7.4), 20 mM N-methylaleimide, 1 mM DTT, 1% (v/v) Triton X-100 and Protease inhibitor cocktail (Nacalai Tesque)]. The cell suspensions were homogenized using a 27 G syringe for at least 10 times and centrifuge at 1000 x *g* for 10 minutes at 4°C. Protein samples were then recovered and stored at -80°C freezer for future use.

Protein samples were next treated with SDS-PAGE electrophoresis using 7.5%, 11.25, and 15% polyacrylamide gel. These separated proteins were then transferred onto an Immobilon-P PVDF membrane (Milipore Corp., M.A) whereby blocking and antibody treatment would be carried out next. Blocking was carried out by incubating the membrane at room temperature for 60 minutes in 5% (w/v) skimmed milk dissolved in TBST (tris-buffered saline) [20 mM Tris-HCl (pH 7.4), 150 mM NaCl, 0.05% (v/v) Tween 20].

Mouse anti-NDUFB8 antibody (complex I) (Abcam, Cambridge, United Kingdom; 1:1000 dilution), mouse anti-SDHB antibody (complex II) (Abcam, Cambridge, United Kingdom; 1:500 dilution), mouse anti-UQCRC2 antibody (complex III) (Abcam, Cambridge, United Kingdom; 1:1000 dilution), mouse anti-cytochrome *c* antibody (Becton Dickinson, Franklin Lakes, New Jersey, USA; 1:200 dilution), mouse anti-cytochrome *c* oxidase sub unit I antibody (complex IV) (Santa Cruz Biotechnology Inc., Dallas, Texas, USA; 1:200 dilution), mouse anti-ATP5A antibody (complex V) (Abcam, Cambridge, United Kingdom; 1:1000 dilution), rabbit anti-PGC-1α (Santa Cruz Biotechnology Inc., Dallas, Texas, USA; 1:200 dilution), and human anti-actin antibody (MP Biomedicals, Santa Ana, CA, USA; 1:200 dilution) which served as internal control, were used in primary antibody treatment. Secondary antibody used in this study were horseradish peroxidase (HRP)-conjugated anti-mouse (Cell Signaling Technology, Beverly, MA, USA) and anti-rabbit IgG (Santa Cruz Biotechnology Inc., Dallas, Texas, USA) concentrate, which were diluted 3000 times in TBST solution. Substrate for HRP used in this study were Western Lightning Chemiluminescent Reagent Plus, Western Lightning Chemiluminescent Reagent Pro (PerkinElmer Life and Analytical Sciences, Waltham, MA, USA), Western Blot Ultra-Sensitive HRP substrate (TaKaRa Bio, Inc., Shiga, Japan). Chemiluminescent were used to quantify protein expression levels

using Lumino Imaging Analyzer LAS-4000 mini (GE Healthcare UK, Amersham Place, England).

Enzymatic activities of cytochrome c oxidase

Measurement of COX activity was carried out by colorimetric analysis using cytochrome *c* oxidase kit (Sigma Aldrich Corporation, Tokyo, Japan). Protein concentration of the extracted mitochondria was determined by the Bradford method. Then, mitochondrial fractions were diluted and adjusted to 100 µg protein / 100 µl with enzyme dilution buffer containing 1 mM n-dodecyl β-D-maltoside. Reduced cytochrome c that reduced by dithiothreitol (DTT) was added to the sample and COX enzymatic activity was measured by following the oxidation of reduced cytochrome *c* at 550 nm. Cytochrome c has a large difference in molar absorptivity at 550 nm between the reduced and oxidized forms (Bery et. al., 1987). Accordingly, the COX activity was calculated based on the absorbance of the oxidation of reduced cytochrome c at pH 7.0 and 25°C. Then, the rate of the oxidation of reduced cytochrome c (1.0 µmol / min) was defined as a unit.

Adenosine triphosphate (ATP) level determination

Cellular ATP level in the myoblasts mitochondria homogenates was extracted with extraction solution in the XL-ATP kit (APRO, Krefeld, Germany) according to the protocol offered by the manufacturer. Cells were first washed twice with PBS after harvested by trypsinization for cell count, followed by centrifugation. ATP in cultured cells was extracted with ATP extraction reagent containing phenol and chloroform. Resulting supernatants called ATP extraction solution, as described previously (Yao *et. al.,* 20018). Samples were then recovered and stored at -20°C freezer for future use. ATP levels in these extracts were determined by measuring the relative luminescence unit (RLU) from samples mixed with assay buffer containing luciferase using Lumino Imaging Analyzer LAS-4000 mini (GE Healthcare UK, Amersham Place, England) and normalized relative to the protein concentrations or live cell numbers. Protein concentration was measured by the Bradford method and live cell numbers were counted by a colorimetric method with trypan blue using Countess II FL Automated Cell Counter (Invitrogen, Tokyo, Japan).

Statistical analysis of data

Data obtained are presented as the means of the replicates ± standard deviation (SD). One-way ANOVA (Tukey's test) was performed for each set of data, and *p* values < 0.05 and < 0.01 were considered statistically significant.

2.3 RESULTS

2.3.1 Effect of exogenous ALA on heme biosynthesis

The concentration of heme was evaluated on mouse myoblast cell. This study is required to observe the effect of import of ALA exogenously in myoblast cells. Cells were administered with 1 mM ALA and incubated 96 hours minutes at 37°C in a 5% CO_2 incubator. The result was recorded and a graph was plotted in **Figure 2.2**. Heme produced in myoblast cells treated with ALA showed a significant increase of 30% compared to the control ($p < 0.05$). The high production of heme in myoblast cells treated with ALA suggested that addition of ALA exogenously induce heme production, in the sense that it demonstrates the accumulation of ALA in cells increased heme biosynthesis.

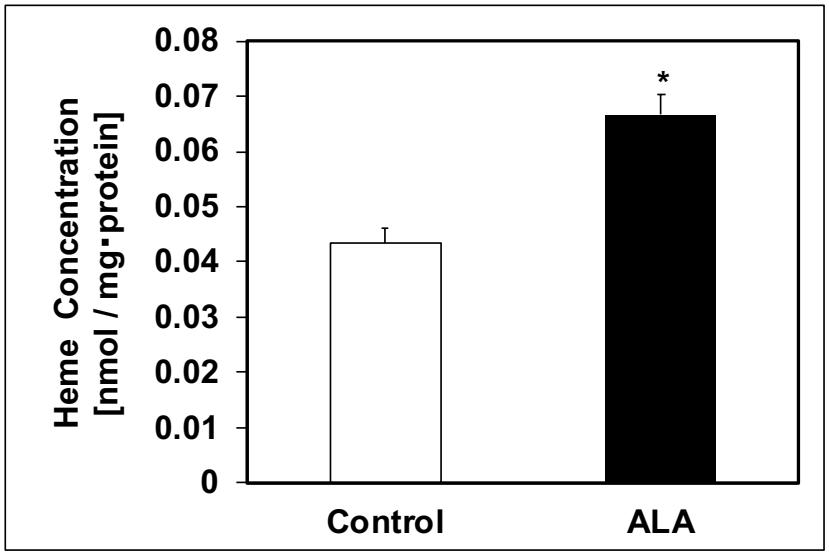

Figure 2.2 Concentration of heme production levels. One-way ANOVA (Tukey's test) was performed for each data set to show significant differences in mean values between treated and untreated samples, *P < 0.05, vs. nontreated control group (Control). Data are expressed as means ± standard deviation (SD) in three independent experiments

2.3.2 ALA increases HO-1 protein expression levels

Heme is degraded by heme oxygenase-1 (HO-1) into iron, carbon monoxide (CO), and biliverdin. HO-1 has been reported to have cytoprotective effects against oxidative stress and inflammation (Li *et. al.,* 2016). Furthermore, it was mentioned that in a mouse fatty liver model and peripheral blood mononuclear cells of healthy humans, the addition of ALA or/and SFC enhanced HO-1 protein expression level (Takeda *et. al.,* 2017; Ito *et. al.,* 2018). Moreover, the recent investigation found that HO-1 protein expression levels were elevated by a combination of ALA and SFC in a concentration-dependent manner in normal human skin fibroblasts (Shimura *et. al.,* 2016). Western blot analysis was conducted to analyze the HO-1 protein expression level (**Figure 2.3** (**A**)). Band intensity ratio analysis from western blot results showed that HO-1 protein expression elevated by ALA (**Figure 2.3** (**B**); $P < 0.01$). Consistent with the heme concentration, HO-1 protein expression levels increased by ALA treatment. Thus, these results showed that the protein expression level of HO-1 dependent on the intracellular heme concentration.

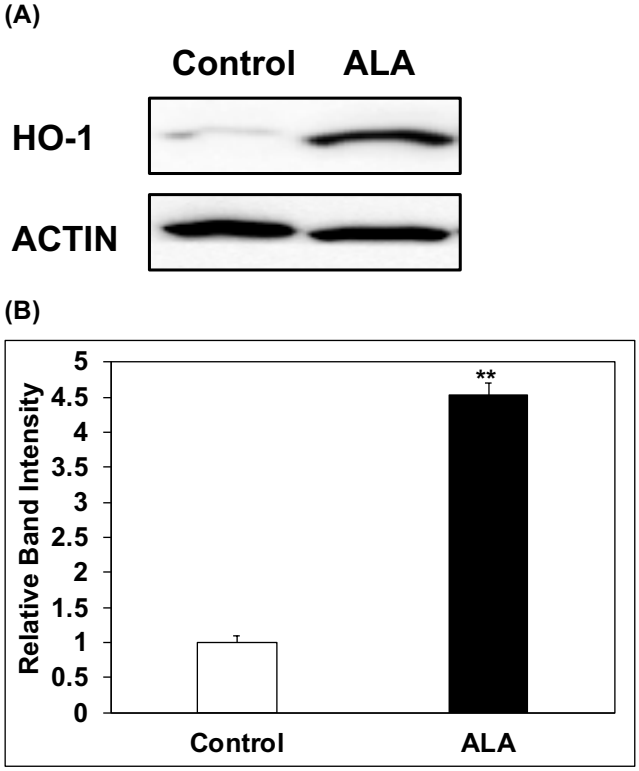

Figure 2.3 Protein levels of HO-1. (**A**) Western blot result of HO-1 protein. (**B**) Graphs of band intensity ratio analysis relative to β-actin are shown. One-way ANOVA (Tukey's test) was performed for each data set to show significant differences in mean values between treated and untreated samples, $^{**}P < 0.01$ vs. nontreated control group (Control). Data are expressed as means ± standard deviation (SD) in three independent experiments

2.3.3 Assessment of mitochondrial content

The expression levels of mitochondrial DNA (mt-DNA) or mt-DNA copy number studies were carried out to identify the mitochondrial content using a modified method Larsen (2012). It was well known that mt-DNA is one of the strongest associated with mitochondrial content (Boushel *et. al.,* 2007; Phielix et. al., 2008). The expression levels of mt-ND1, mt-COX1, and COX2 as the representative of mt-DNA were studied in myoblast cell line in the presence and absence of 1 mM ALA and incubated 96 hours at 37°C in a 5% CO_2 incubator. The samples were then collected and were analyzed using real-time PCR. Results of mt-DNA expression levels of these genes using real-time PCR were presented in **Figure 2.4**.

Data from qRT-PCR exhibited there are no significant differences of mt-DNA expression levels of mt-ND1, mt-COX1, and mt-COX2 in the addition of ALA compared to control. The results here also expressed that the addition of ALA did not affect mitochondrial content in myoblast cells.

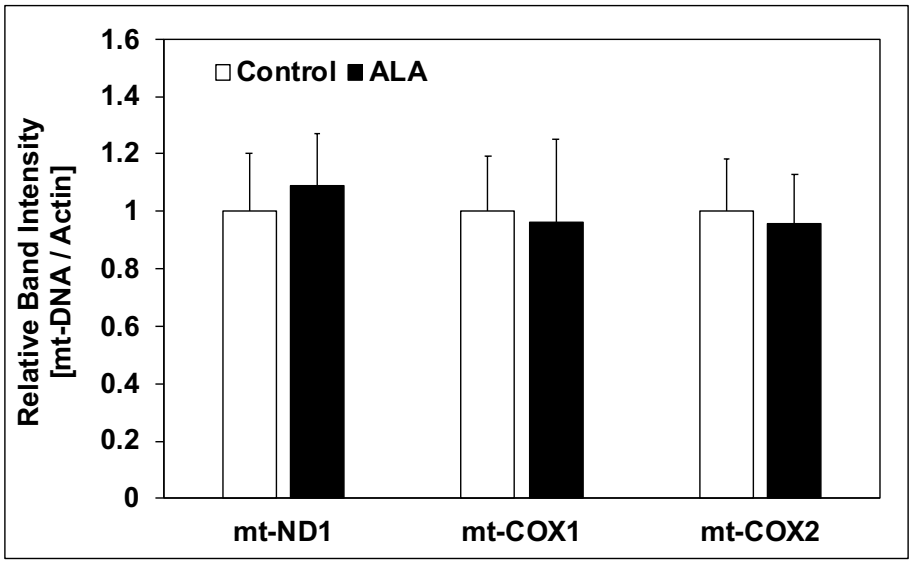

Figure 2.4 Mitochondrial content analysis. Relative expression levels of mtDNA (mt-ND1, mt-COX1, and mt-COX2) copy number by real-time qPCR analysis.

2.3.4 Mitochondrial biogenesis analysis

Mitochondrial biogenesis can be defined as the growth and division of pre-existing mitochondria (François *et. al.,* 2014). The relative mRNA expression levels of transcription factors affecting mitochondrial biogenesis namely TFAM, NRF1, and NRF2 (Scarpulla, 2006) as shown in **Figure 2.5** were analyzed to investigate the effects of administration of ALA on the mitochondrial biogenesis. In addition, the

expression level of PGC-1α, a transcriptional regulator for genes involved in mitochondrial biogenesis was also examined. mRNA expression levels were studied in myoblast cells in the presence and absence of 1 mM ALA and incubated 96 hours minutes at 37°C in a 5% CO_2 incubator. The samples were then collected and were analyzed using quantitative reverse transcriptase-polymerase chain reaction (qRT-PCR). Results of mRNA expression levels of these genes using qRT-PCR were shown in **Figure 2.6**.

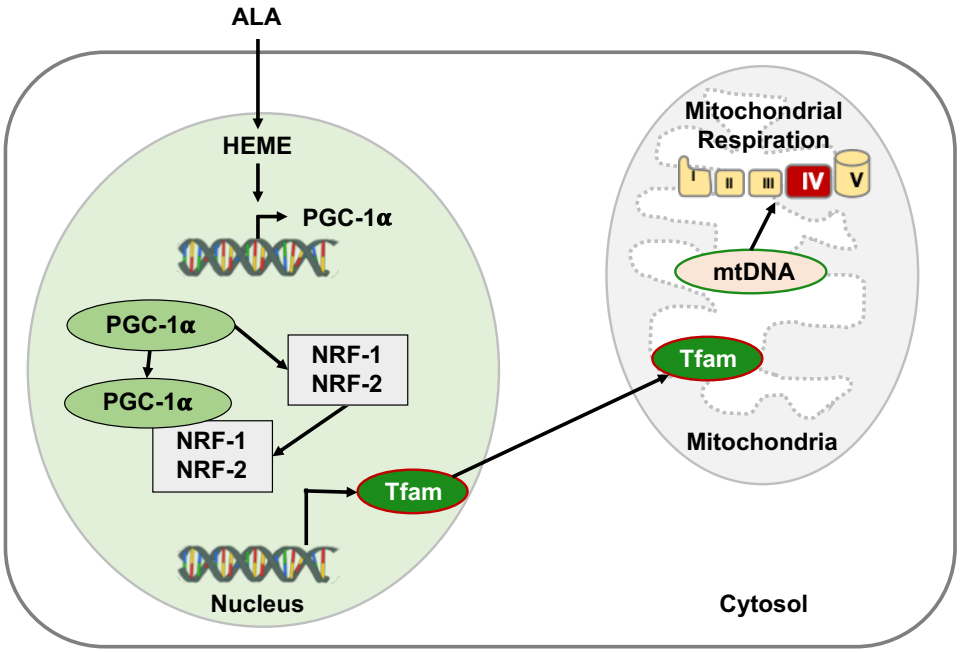

Figure 2.5 Conceptual diagram of genes involved in mitochondrial biogenesis and how exogenous ALA is involved

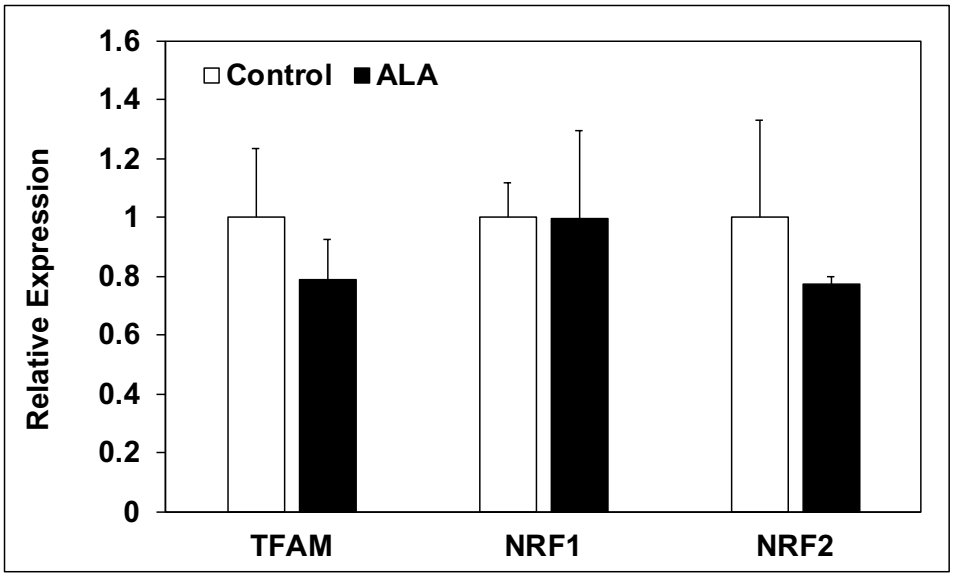

Figure 2.6 Relative mRNA-expression of mitochondrial biogenesis related genes (TFAM, NRF1, and NRF2)

Findings from qRT-PCR presented that mRNA expression of TFAM and NRF1 which mediate mitochondrial biogenesis were similar in the addition of ALA and in the control. In addition, mRNA expression of NRF2 that facilitate cellular responses to oxidative stress did not change following ALA administration. In agreement, there is no different in mRNA expression level of *PGC-1α* which regulates the genes involved in mitochondrial biogenesis as shown in **Figure 2.7** (**A**). These findings suggested that the addition of ALA did not affect the mitochondrial biogenesis.

Furthermore, the protein expression level of PGC-1α was also determined. Results of the protein expression level of PGC-1α who has a responsibility as a master regulator for genes involved in mitochondria biogenesis were showing as electropherogram in **Figure 2.7** (**B**) and band intensity graphs were plotted as in **Figure 2.7** (**C**) Western blotting results revealed very similar and consistent with the results obtained by qRT-PCR analysis. There is no significant different in the protein expression level of PGC-1α in addition of ALA and in the control. These findings exhibit the addition of ALA in myoblast cells did not alter the mitochondrial biogenesis.

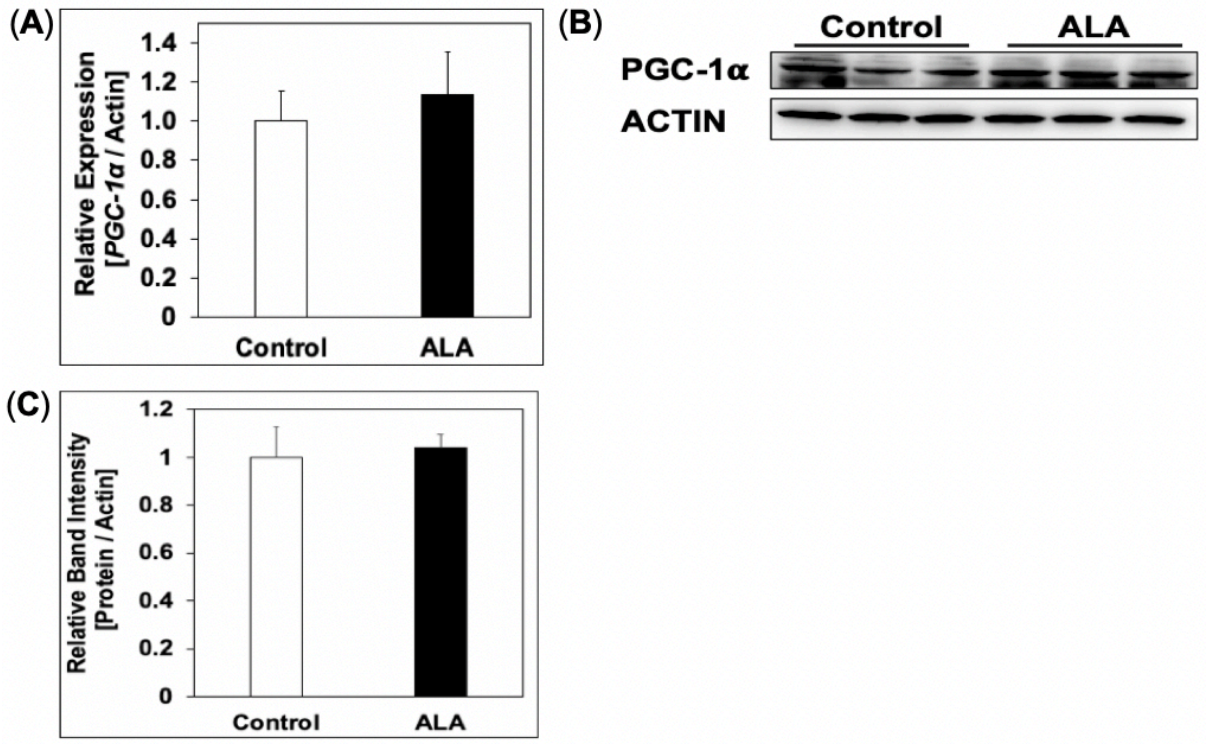

Figure 2.7 Mitochondrial biogenesis analysis. (**A**) Relative mRNA-expression level of *PGC-1α*. (**B**) Western blot result of PGC-1α protein. (**C**) Graphs of band intensity ratio analysis relative to β-actin are shown.

2.3.5 Heme triggers the alterations of the electron transport chain protein expression levels

The protein expression levels of the electron transport chain were studied to evaluate the effects of increasing heme biosynthesis on the oxidative phosphorylation system. The protein expression levels of cytochrome *c* and electron transport chain were observed in the presence or absence of 1 mM ALA addition for 96 hours at 37°C in a 5% CO_2 incubator. The samples were then collected and being analyzed by western blotting. Results of the protein expression level of these membrane protein complexes of the electron transport chain were showing as electropherogram in **Figure 2.8** (**A**) and band intensity graphs were plotted as in **Figure 2.8** (**B**).

Protein expression levels of the electron transport chain were observed in myoblast cells with the addition of ALA compared to the control. Protein expression levels of complex I and complex II were found to be significantly decreased by 60% and 40% respectively in the presence of ALA ($p < 0.05$). These data might be attributed with both complex I and complex II have multiple iron-sulfur clusters, it has the possibility to provide a source of iron ion, enhanced heme biosynthesis further in the presence of ALA. Therefore, both complex I and complex II protein expression levels were decreased with the addition of ALA and followed by increasing of heme biosynthesis. On the one hand, it was found out that there was no significant difference in the protein expression level of complex V and complex III. On the other hand, the current results presented that the protein expression levels of cytochrome *c* and complex IV were significantly increased about 35% and 50% respectively with the addition of ALA ($p < 0.05$). The results of protein expression levels of the electron transport chain here suggested that addition of ALA stimulates the oxidative phosphorylation system by upregulation mitochondria respiratory chain cytochrome *c* oxidase, it indicated by a significant increase.

(A)

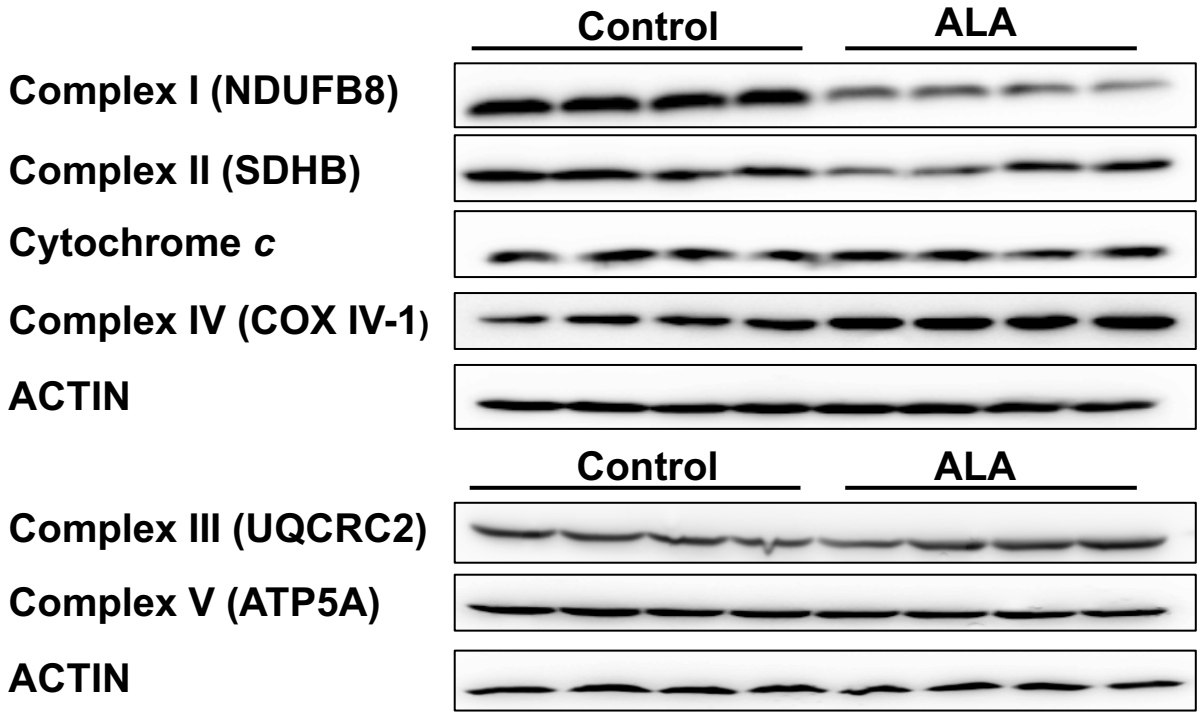

(B)

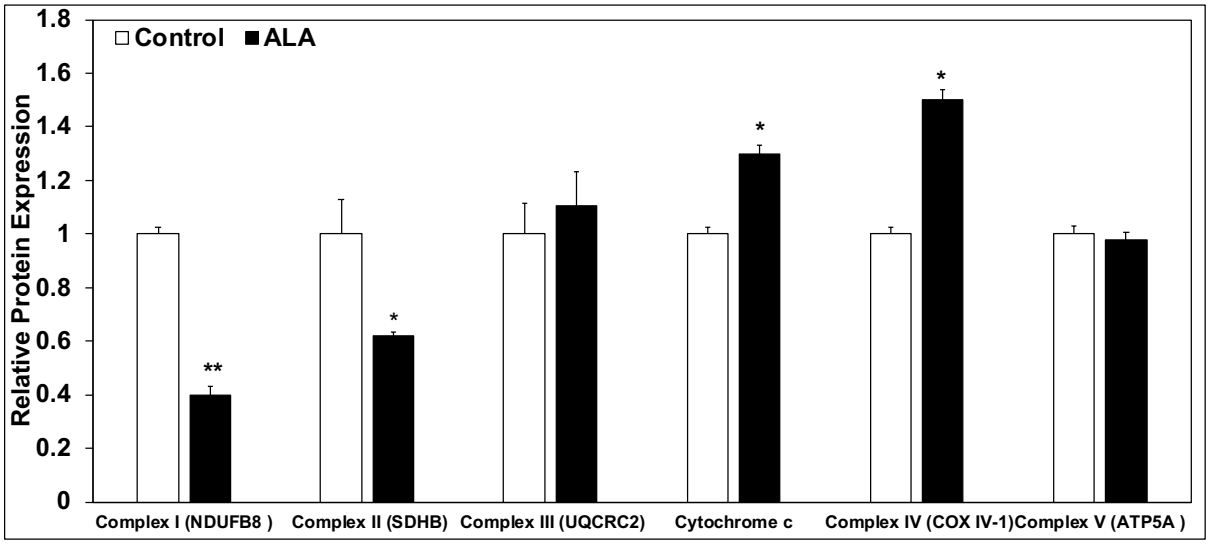

Figure 2.8 Protein levels of mitochondrial OXPHOS. (**A**) The protein expression levels of mitochondrial OXPHOS were measured by Western blot. (**B)** Graphs of band intensity ratio analysis relative to β-actin are shown. One-way ANOVA (Tukey's test) was performed for each data set to show significant differences in mean values between treated and untreated samples, **P* < 0.05, ***P* < 0.01 vs. nontreated control group (Control). Data are expressed as means ± standard deviation (SD) in three independent experiments.

2.3.6 COX activity measurement

ALA has been reported to increase COX activity by 40% in the liver of C57BL/6N mice (Sugiyama *et. al.,* 2014). To further study this effect, mitochondrial fractions extracted from ALA administered myoblast cells were used to measure COX activity. COX activity was measured by quantifying the oxidation of reduced cytochrome *c*. COX activity significantly increased in the presence of ALA (**Figure 2.9**; P < 0.01). This result indicates that an increase in mitochondrial OXPHOS system capacity, which may suggest an increase in mitochondrial activity.

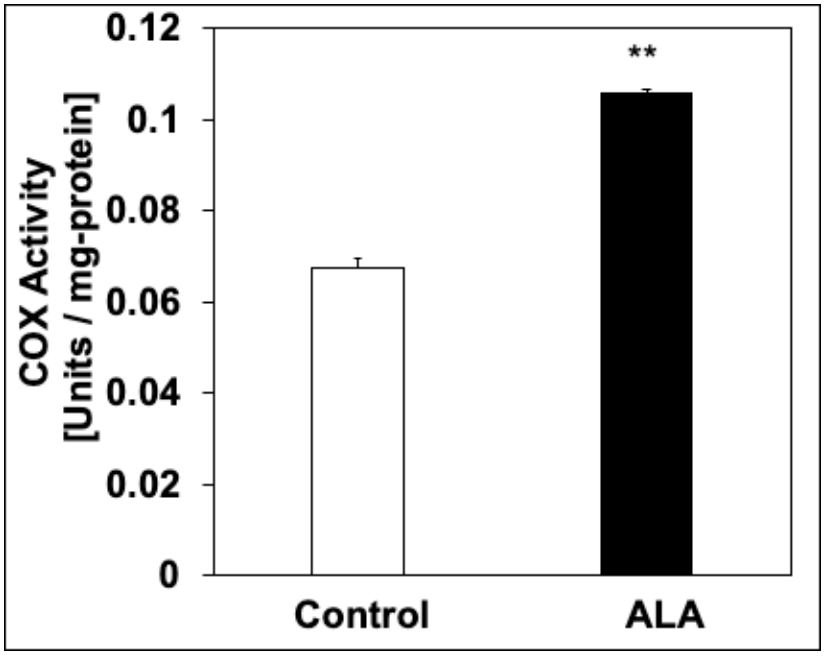

Figure 2.9 Enzymatic activity of COX per mg protein. One-way ANOVA (Tukey's test) was performed for each data set to show significant differences in mean values between treated and untreated samples, ***P* < 0.01 vs. nontreated control group (Control). Data are expressed as means ± standard deviation (SD) in three independent experiments.

2.3.7 Quantification of ATP production levels

In the previous report, the ATP production level was significantly higher in ALA administered mouse liver cells (Ogura *et. al.,* 2011). To further confirm this, was added to the cells. Mitochondrial fractions extracted from each treatment were used to measure the total ATP production level. Supporting the occurrence of an increase in COX activity, total ATP production level strongly promoted after treatment with ALA (**Figure 2.10**; P < 0.05). These data show that the addition of ALA increased

mitochondrial activity through stimulates the mitochondrial OXPHOS system by activating COX activity.

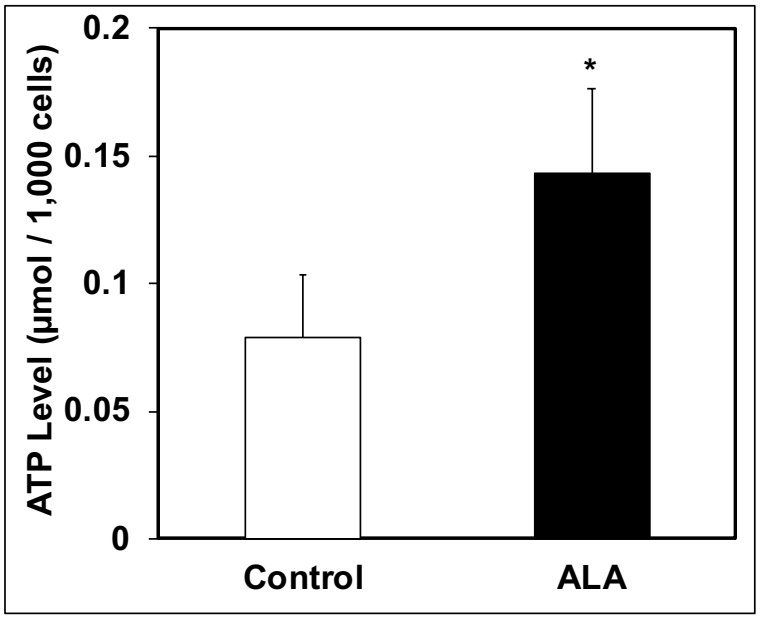

Figure 2.10 ATP production levels. One-way ANOVA (Tukey's test) was performed for each data set to show significant differences in mean values between treated and untreated samples, $^{**}P < 0.01$ vs. nontreated control group (Control). Data are expressed as means ± standard deviation (SD) in three independent experiments.

2.4 DISCUSSION

Mitochondria in cells are very important essential organelles for maintaining homeostasis system, including heme biosynthesis in the organism. It has been well known that abnormalities in number of mitochondria and mitochondrial dysfunctions are the key player in variety of disease and human abnormalities/disorders (Wallace, 2009; Stöckl *et. al.*, 2006; Short *et. al.,* 2005; Conley, 2000) such as aging (Patel, 2002; Payne & Chinnery, 2015; Srivasta, 2017; Trifunovic & Larsson, 2008; Sun *et. al.,* 2016), diabetes (Gerbitz *et. al.,* 1996; Parish & Petersen, 2005; Ritov *et. al.,* 2005), cancer, and neurodegenerative diseases including Parkinson's (Mizuno *et. al.,* 1989), Huntington's and Alzheimer diseases (Candeias *et. al.,* 2012; Sheng *et. al.,* 2012). In addition, reduction in mitochondrial respiration has also reported in cancer that leading cause of death. Furthermore, in healthy people, with the aging process, the decrease in the number of mitochondria, mitochondrial biogenesis capacity, and the associated protein of electron transfer system in electron transport chain were reported to be decreased (Short, 2005; Conley, 2000).

From all of the facts and growing pieces of evidence explained above, it is really important to develop a health care treatment to prevent the dysfunction of mitochondria and keep maintain its functions. In this study, ALA is proposed to use because it has attracted much attention for its great potential applications in the fields of medicine. This study also shows the schematic illustration of the addition of ALA in cells and its possibilities to make some effects on the oxidative phosphorylation system, including in the electron transfer in the electron transport chain.

This present study revealed that the protein expression levels of the electron transport chain in myoblast cells were quantified and tabulated in **Table 2.4**. It is clearly seen that protein expression levels of cytochrome c and complex IV were significantly increased by 35% and 50%, respectively, with the addition of ALA. Based on these findings, it is strongly believed that the addition of ALA elevated the oxidative phosphorylation system.

Table 2.4 Summary on protein expression levels of electron transport chain

Complex I & II	↓
Complex III & V	No changes
Cytochrome *c* & Complex IV	↑

The results of mitochondrial content studied mt-DNA copy number analysis, it revealed there are no significant differences were observed between samples treated with ALA compared to the control, which means mitochondrial content in both samples relatively equal. Thus, addition of ALA did not affect the mitochondrial content in myobloast cells. Following the unchanged on mitochondrial content after ALA administered, we hypothesized that mitochondrial biogenesis would not change as well. Using qRT-PCR analysis, we demonstrated the relative mRNA-expression of mitochondrial biogenesis related genes namely TFAM, NRF1, and NRF2 & PGC-1α were similar in the absence and presence of ALA. Supporting mRNA results, the protein expression level of PGC-1α did not alter after the addition of ALA.

All in all, the data in this study reveals that the addition of ALA in myoblast (C2C12) cells caused upregulation on heme biosynthesis. The study also

demonstrated that ALA stimulated the oxidative phosphorylation system by upregulation the mitochondria respiration chain cytochrome *c* oxidase or complex IV. Moreover, the ATP production level was significantly increase after the administration of ALA. Nonetheless, the presence of ALA alone did not affect mitochondrial content and mitochondrial biogenesis.

CHAPTER 3
5-AMINOLEVULINIC ACID AND SODIUM FERROUS CITRATE ENHANCED MITOCHONDRIAL ACTIVITIES IN MYOBLAST CELLS

3.1 INTRODUCTION

Mitochondria are rod-shaped that can be considered the power generators of the cell through the oxidative phosphorylation. Mitochondria perform pivotal cellular reactions, including the regulation of cell death, calcium metabolism and the production of reactive oxygen species (Spinazzi *et. al.,* 2012). Unit of energy in cells is ATP and the main synthesis pathway to aerobic organisms is oxidative phosphorylation. During OXPHOS, electrons are transferred from electron donors to electron acceptors such as oxygen, in redox reactions. These redox reactions generate energy, which is used to convert adenosine diphosphate (ADP) to ATP. These redox reactions are carried out by a series of protein complexes embedded in the inner mitochondrial membrane called electron transport chain.

Dysfunction of mitochondria is notorious as a key player in a variety of human disorders, such as aging, diabetes, cancer, and neurodegenerative diseases including Parkinson's, Huntington's and Alzheimer diseases (Allen *et. al.,* 2018; Gris, 2009; Gris, 2013). In the previous experiment, it was reported that COX activities in mitochondria were lower in tumors cells compared to normal cells, it can be categorized as defects in the oxidative phosphorylation (Sugiyama *et. al.,* 2012; Sugiyama *et. al.,* 2013). Among those findings, it also revealed that the addition of ALA caused an increase in COX activity both *in vivo* and *in vitro* based on experiments carried out by Sugiyama (2011). All of the previous experiments demonstrated that ALA administered both *in vitro* and *in vivo* stimulates oxidative phosphorylation by upregulation of the mitochondrial respiratory chain cytochrome *c* oxidase.

The effect of ALA on mitochondrial activity was studied in the previous chapter, and it was reported that ALA increased mitochondrial activity by stimulating the OXPHOS system. To further increase the mitochondrial activity, SFC is used. Since SFC is the iron ion provider, that has the possibility to increase heme biosynthesis and HO-1 protein expression level. Moreover, it also has the potential to up-regulate the expression levels of heme protein and eventually improve mitochondrial activity by stimulating the oxidative phosphorylation system.

Additionally, during the synthesis of heme, ALA immediately is converted to PpIX via several steps. After that, heme is formed by the insertion of iron ion to PpIX; SFC can provide the free iron ion for this process. Interestingly, mitochondrial respiration chain complex IV and cytochrome *c* are heme proteins; and it is sensitive to changes

in heme concentration in mitochondria. Previous studies have reported that exogenously addition of ALA increases heme biosynthesis (Miura *et. al.,* 2015), and it is possible to increase mitochondrial activity. Furthermore, ALA combined with SFC in healthy humans increased heme oxygenase-1 (HO-1) (Takeda *et.al.,* 2017; Ito *et. al.,* 2018). This study aims to investigate the effect of ALA and SFC on mitochondrial activity in myoblast cells. Moreover, this study also focused on analyzing the effect of ALA, SFC, and ALA combined with SFC on the protein that contains iron-sulfur (Fe-S) clusters in mitochondria in myoblast cells. Myoblast cells are mouse skeletal muscle cell lines. This cell is a suitable model for assessing mitochondrial activity because muscle cells rely on OXPHOS to produce energy (McMahon *et. al.,* 1994; Chung *et, al.,* 2007; Chung *et,.al,* 2008). Therefore, in this chapter, the effect of exogenous addition of ALA and SFC on mitochondrial activity in myoblast cells could be observed as illustrated in **Figure 3.1**.

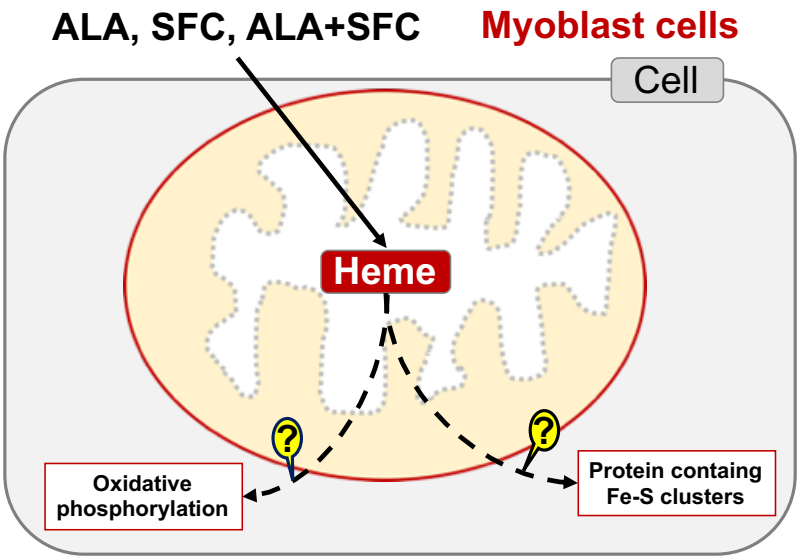

Figure 3.1 Conceptual diagram of addition of exogenous ALA, SFC, and ALA+SFC in myoblast cells.

3.2 MATERIALS & METHODS

Chemicals

DMEM-high glucose medium, DMEM-low glucose medium, and antibiotic-antimycotic mixed stock medium (ABAM) were purchased from Nacalai Tesque (Kyoto, Japan). Fetal bovine serum (FBS) and horse serum (HS) were purchased from Invitrogen (Carlsband, California, USA). Aminolevulinic acid (ALA) was purchased from Cosmo Bio Co. Ltd. (Tokyo, Japan).

Cell culture

Mouse myoblast cells, namely the C2C12 cell line, were obtained from RIKEN, Japan. Myoblast cells were cultured in DMEM-high glucose culture medium. Cells were incubated and followed by addition of 10% FBS and 10% ABAM, at 37°C in a 5% CO_2 incubator. When cells were reached 70% – 80% confluency previous medium was replaced with differentiation medium, DMEM-low glucose followed by addition of 2% HS and 10% ABAM. Differentiation medium was replaced with fresh ones every 48 hours for 6 days. Cell number for seeding in various experiments is tabulated in **Table 3.1**.

Table 3.1 Amount of cell seeded for each experiment

Experiments	Seeding cell number (cells / well)
Heme production level	0.5×10^6 cells
HO-1 protein expression level	
Protein expression level of electron transport chain	
Protein expression level containing Fe-S clusters in mitochondria	
COX activity measurement	0.5×10^7 cells
ATP production level quantification	

Heme production quantification using High performance Liquid Chromatography (HPLC)

Cells were seeded in 35 mm dishes and incubated at 37°C in a 5% CO_2 incubator to reach confluency then differentiated to be myotube. Experiments were carried out in triplicates per sample. Addition of ALA was carried out and cells were further incubated under the same condition for the next 96 hours. In order to quantify extracellular heme, medium with serum should be avoided but not if only quantify intracellular heme. Cells on 35 mm dishes first were placed on ice and washed with cold PBS 3 times. Cells were lysed with 150 µL 0.1 N NaOH. a volume of 50 µL of cell suspension from each sample were taken out and added into a new 1.5 mL centrifuge tube containing 150 µL of (1 : 9; 1 M CH_3COONH_3, 12.5% acetonitrile, pH 5.2 : 50 mM CH_3COONH_3, 80% acetonitrile, pH 5.2). Cells suspension then underwent

centrifugation under 10,000 x *g* for 10 minutes. Supernatants were recovered and pellets were discarded.

HPLC analysis of heme was carried out using Type Prominence System (Shimadzu Manufacturing Co., Kyoto, Japan) equipped with reverse phase C18 column (CAPCELL PAK, C18, SG300, 5 µm, 4.6 mm x 250 mm, Osaka Soda Co. Ltd., Osaka) while maintaining at temperature of 40°C. Mobile phase A, comprising 1 M ammonium acetate solution containing 12.5% acetonitrile (adjusted to pH 5.2), and mobile phase B made up of 50 mM ammonium acetate solution containing 80% acetonitrile, were used in elution of heme. 50% mobile phase B was first directed at a flow rate of 1.0 mL / min for 10 minutes following by driving mobile phase B into column from a linear gradient ranging from 90% for 10 minutes and finally 90% mobile phase B at a flow rate 2.0 mL / min for another 10 minutes elution program. Protein concentration of each samples were determined using Bradford's method using Quickstart Bradford 1 x Dye reagent (Biorad laboratories, Inc., Hercules, California, USA).

Western blotting

Western blotting experiments were carried out to quantify the expression level of proteins in cell using modified method based on Kogot-Levin *et. al.* (2016). Cells were first washed with PBS (-), followed by addition Lysis Buffer A [50 mM Tris-HCl (pH 7.4), 20 mM N-methylaleimide, 1 mM DTT, 1% (v/v) Triton X-100 and Protease inhibitor cocktail (Nacalai Tesque)]. The cell suspensions were homogenized using a 27 G syringe for at least 10 times and centrifuge at 1000 x *g* for 10 minutes at 4°C. Protein samples were then recovered and stored at -80°C freezer for future use.

Protein samples were next treated with SDS-PAGE electrophoresis using 7.5% and 11.25 polyacrylamide gel. These separated proteins were then transferred onto an Immobilon-P PVDF membrane (Milipore Corp., M.A) whereby blocking and antibody treatment would be carried out next. Blocking was carried out by incubating the membrane at room temperature for 60 minutes in 5% (w/v) skimmed milk dissolved in TBST [20 mM Tris-HCl (pH 7.4), 150 mM NaCl, 0.05% (v/v) Tween 20].

Mouse anti-cytochrome *c* oxidase sub unit I antibody (complex IV) (Santa Cruz Biotechnology Inc., Dallas, Texas, USA; 1:200 dilution), and human anti-actin antibody (MP Biomedicals, Santa Ana, CA, USA; 1:200 dilution) which served as internal control,

were used in primary antibody treatment. Secondary antibody used in this study were horseradish peroxidase (HRP)-conjugated anti-mouse (Cell Signaling Technology, Beverly, MA, USA) and anti-rabbit IgG (Santa Cruz Biotechnology Inc., Dallas, Texas, USA) concentrate, which were diluted 3000 times in TBST solution. Substrate for HRP used in this study were Western Lightning Chemiluminescent Reagent Plus, Western Lightning Chemiluminescent Reagent Pro (PerkinElmer Life and Analytical Sciences, Waltham, MA, USA), Western Blot Ultra-Sensitive HRP substrate (TaKaRa Bio, Inc., Shiga, Japan). Chemiluminescent were used to quantify protein expression levels using Lumino Imaging Analyzer LAS-4000 mini (GE Healthcare UK, Amersham Place, England).

Enzymatic activities of cytochrome *c* oxidase

Measurement of COX activity was carried out by colorimetric analysis using cytochrome *c* oxidase kit (Sigma Aldrich Corporation, Tokyo, Japan). Protein concentration of the extracted mitochondria was determined by the Bradford method. Then, mitochondrial fractions were diluted and adjusted to 100 μg protein / 100 μl with enzyme dilution buffer containing 1 mM n-dodecyl β-D-maltoside. Reduced cytochrome *c* that reduced by dithiothreitol (DTT) was added to the sample and COX enzymatic activity was measured by following the oxidation of reduced cytochrome *c* at 550 nm. Cytochrome *c* has a large difference in molar absorptivity at 550 nm between the reduced and oxidized forms (Bery *et. al.,* 1987). Accordingly, the COX activity was calculated based on the absorbance of the oxidation of reduced cytochrome *c* at pH 7.0 and 25°C. Then, the rate of the oxidation of reduced cytochrome *c* (1.0 μmol / min) was defined as a unit.

Enzymatic activities of cytochrome *c* oxidase

Measurement of COX activity was carried out by colorimetric analysis using cytochrome *c* oxidase kit (Sigma Aldrich Corporation, Tokyo, Japan). Protein concentration of the extracted mitochondria was determined by the Bradford method. Then, mitochondrial fractions were diluted and adjusted to 100 μg protein / 100 μl with enzyme dilution buffer containing 1 mM n-dodecyl β-D-maltoside. Reduced cytochrome *c* that reduced by dithiothreitol (DTT) was added to the sample and COX enzymatic activity was measured by following the oxidation of reduced cytochrome *c*

at 550 nm. Cytochrome *c* has a large difference in molar absorptivity at 550 nm between the reduced and oxidized forms (Bery *et. al.,* 1987). Accordingly, the COX activity was calculated based on the absorbance of the oxidation of reduced cytochrome *c* at pH 7.0 and 25°C. Then, the rate of the oxidation of reduced cytochrome *c* (1.0 µmol / min) was defined as a unit.

Cytotoxicity assay

Cytotoxicity level of specific reagents that used in various purposes was carried out by colorimetric analysis using 3-[4,5-dimethylthiazol-2-yl]-2,5-diphenyl tetrazolium bromide (MTT). Cells were grown in 96 well microplates, a specific chemical was added and dilution series was made by shift each 100 µL to the right lane, after that 96 well microplates was incubated for 96 hours at 37°C in a 5% CO_2 incubator. A 10 µL mixed PBS and MTT was added in each well then incubated for 4 hours at 37°C in a 5% CO_2 incubator, 100 µL 10% SDS was added then incubated for another 24 hours. Absorbance were measured in 2 different wavelengths at 570 nm and 650 nm using Multiskan FC (Thermo Fischer, Massachusetts, USA). The obtained data was analyzed using Microsoft Excel program.

Adenosine triphosphate (ATP) level determination

Cellular ATP level in the myoblast mitochondria homogenates was extracted with extraction solution in the XL-ATP kit (APRO, Krefeld, Germany) according to the protocol offered by the manufacturer. Cells were first washed twice with PBS after harvested by trypsinization for cell count, followed by centrifugation. ATP in cultured cells was extracted with ATP extraction reagent containing phenol and chloroform. Resulting supernatants called ATP extraction solution, as described previously (Yao *et. al.,* 20018). Samples were then recovered and stored at -20°C freezer for future use. ATP levels in these extracts were determined by measuring the relative luminescence unit (RLU) from samples mixed with assay buffer containing luciferase using Lumino Imaging Analyzer LAS-4000 mini (GE Healthcare UK, Amersham Place, England) and normalized relative to the protein concentrations or live cell numbers. Protein concentration was measured by the Bradford method and live cell numbers were counted by a colorimetric method with trypan blue using Countess II FL Automated Cell Counter (Invitrogen, Tokyo, Japan).

Statistical analysis of data

Data obtained are presented as the means of the replicates ± standard deviation (SD). One-way ANOVA (Tukey's test) was performed for each set of data, and p values < 0.05 and < 0.01 were considered statistically significant.

3.3 RESULTS

3.3.1 Intracellular heme production levels

ALA is the heme precursor in the PpIX biosynthesis pathway that leads to heme production. ALA, SFC, and ALA+SFC have previously been reported to enhance heme production. To further clarify this effect, intracellular heme levels were measured. **Figure 3.2** shows that ALA and SFC increases intracellular heme significantly (**Figure 3.2**; $P < 0.05$); furthermore, the escalation was more evident in ALA+SFC (**Figure 3.2**; $P < 0.01$). To conclude, the addition of ALA increased PpIX biosynthesis and led to increased intracellular heme levels. Alongside the existence of ALA, SFC as a source of iron ions was further induced by heme biosynthesis.

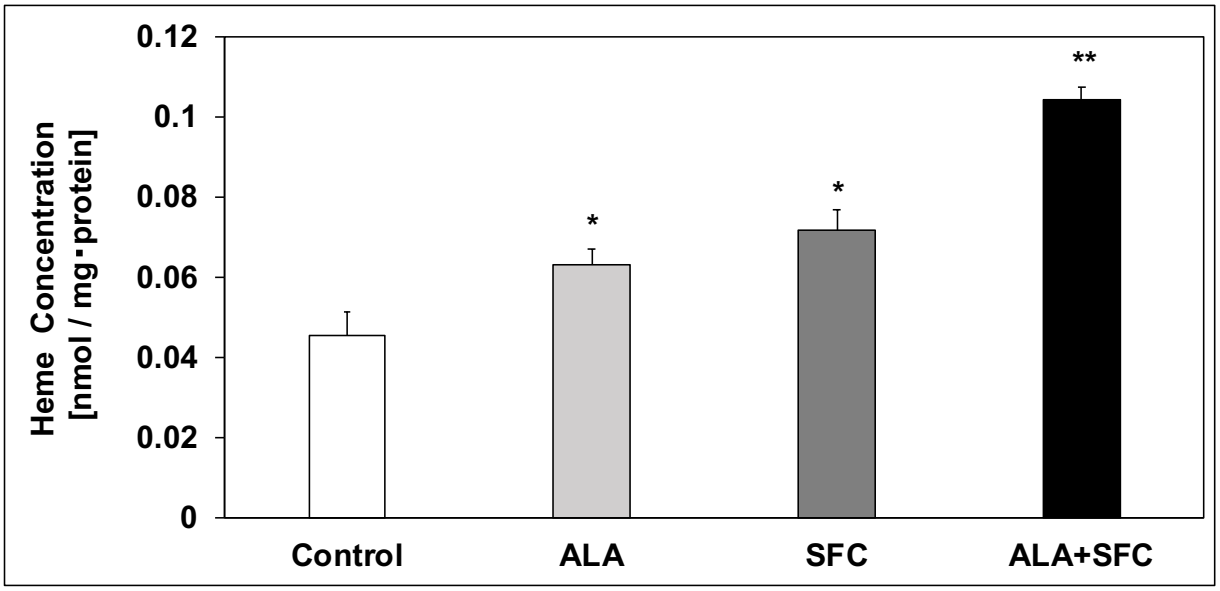

Figure 3.2 Concentration of heme production levels. One-way ANOVA (Tukey's test) was performed for each data set to show significant differences in mean values between treated and untreated samples, *$P < 0.05$, **$P < 0.01$ vs. nontreated control group (Control). Data are expressed as means ± standard deviation (SD) in three independent experiments

3.3.2 HO-1 protein expression levels

Western blot was performed to analyze the HO-1 protein expression level. Band intensity ratio analysis from western blot results showed that HO-1 protein expression

was elevated by the addition of ALA and SFC as shown in **Figure 3.3**. Thus, these results showed that the protein expression level of HO-1 is in line and consistent with the intracellular heme concentration.

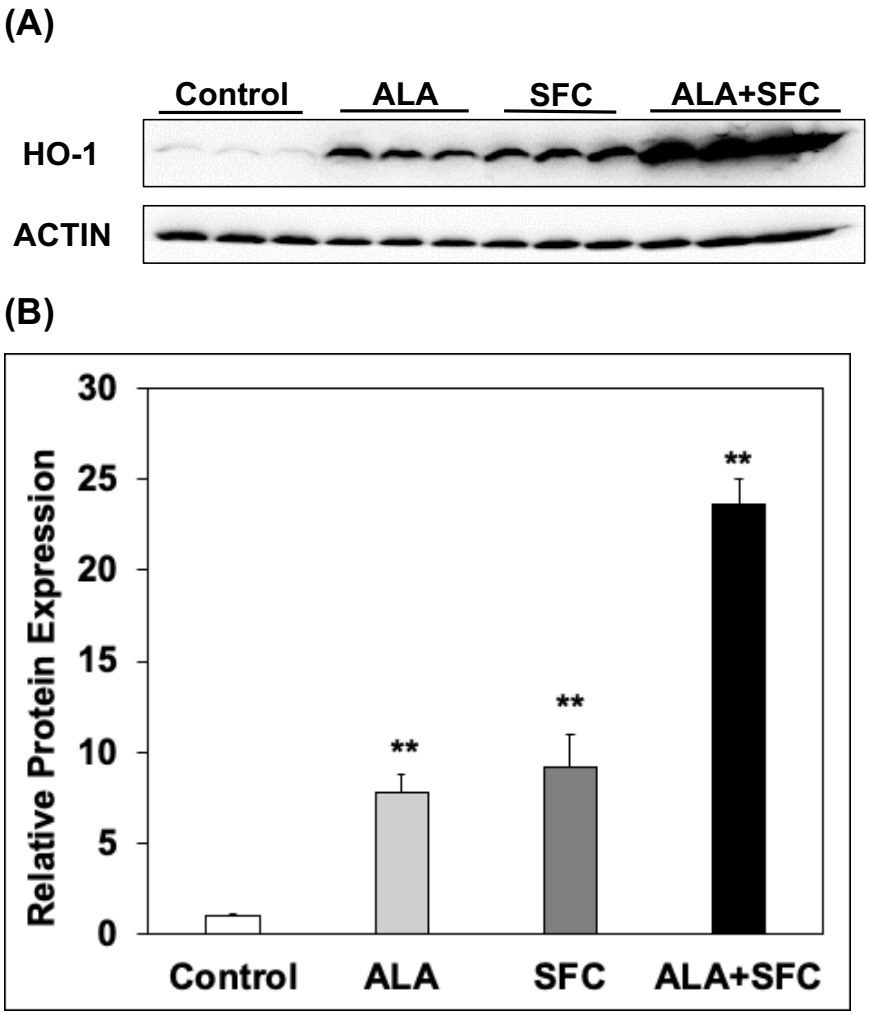

Figure 3.3 Protein levels of HO-1. (**A**) Western blot result of HO-1 protein. (**B**) Graphs of band intensity ratio analysis relative to β-actin are shown. One-way ANOVA (Tukey's test) was performed for each data set to show significant differences in mean values between treated and untreated samples, **P* < 0.05, ***P* < 0.01 vs. nontreated control group (Control). Data are expressed as means ± standard deviation (SD) in three independent experiments

3.3.3 ETC protein expression levels

Heme is synthesized through the porphyrin pathway, in which ALA is the precursor. Then, ALA is converted into PpIX. Lastly, the insertion of ferrous ions then produces heme, while SFC can provide the source of free iron ions. Heme functions as a protein-bound prosthetic group in mitochondrial OXPHOS complex IV and cytochrome *c*. A further effect of ALA on mitochondrial OXPHOS protein was studied by Western blot analyses (**Figure 3.4** (**A**)). The protein expression of

cytochrome *c* and complex IV were significantly up-regulated following the administration of ALA and ALA+SFC (**Figure 3.4** (**B**); $P < 0.05$). Whereas the addition of SFC increases complex IV only (**Figure 3.4** (**B**); $P < 0.05$). On the one hand, complex I and complex II protein (both have iron-sulfur clusters) expression levels were significantly down-regulated after treatment with ALA (**Figure 3.4** (**B**); $P < 0.01$). Contrarily, it was notably up-regulated after treatment with SFC (**Figure 3.4** (**B**); $P < 0.05$) and recovered back to the control level in ALA+SFC. On the other hand, ALA, SFC, and ALA+SFC did not significantly impact complex III and complex V protein expression levels (**Figure 3.4** (**B**)). Taken together, hemeproteins in mitochondrial OXPHOS have shown a remarkable increase after the addition of ALA and ALA+SFC, where SFC only increased the complex IV. Moreover, SFC significantly increased the OXPHOS protein expression containing iron-sulfur clusters in mitochondria. However, it was remarkably down-regulated in the presence of ALA.

(A)

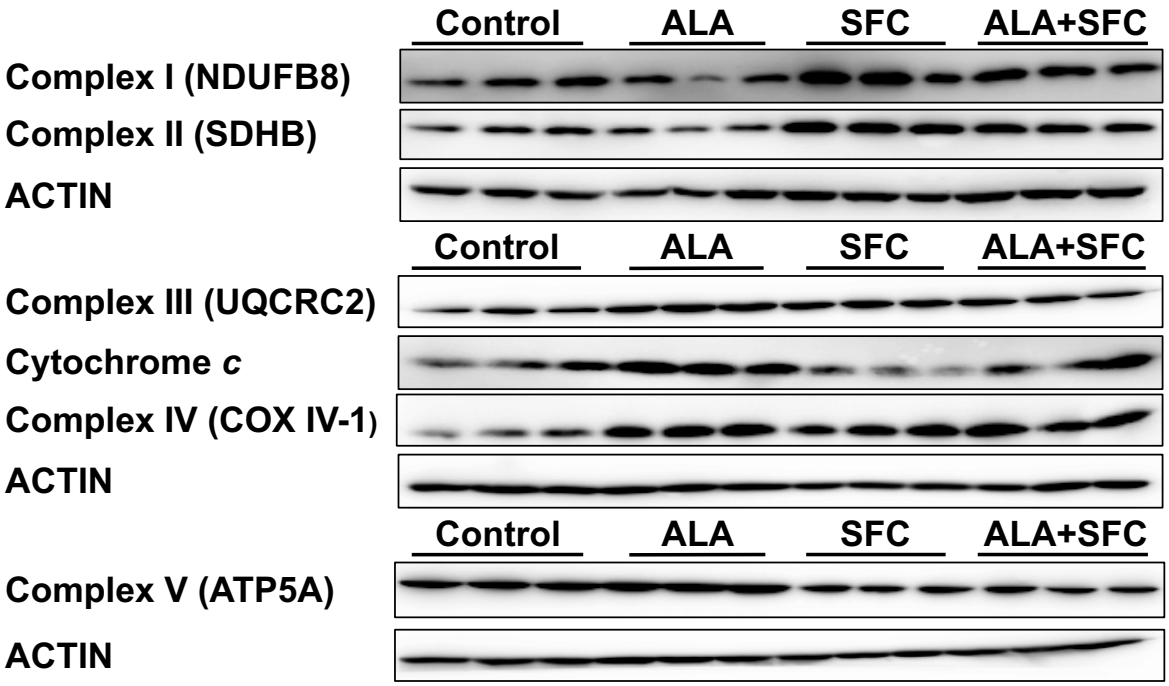

(B)

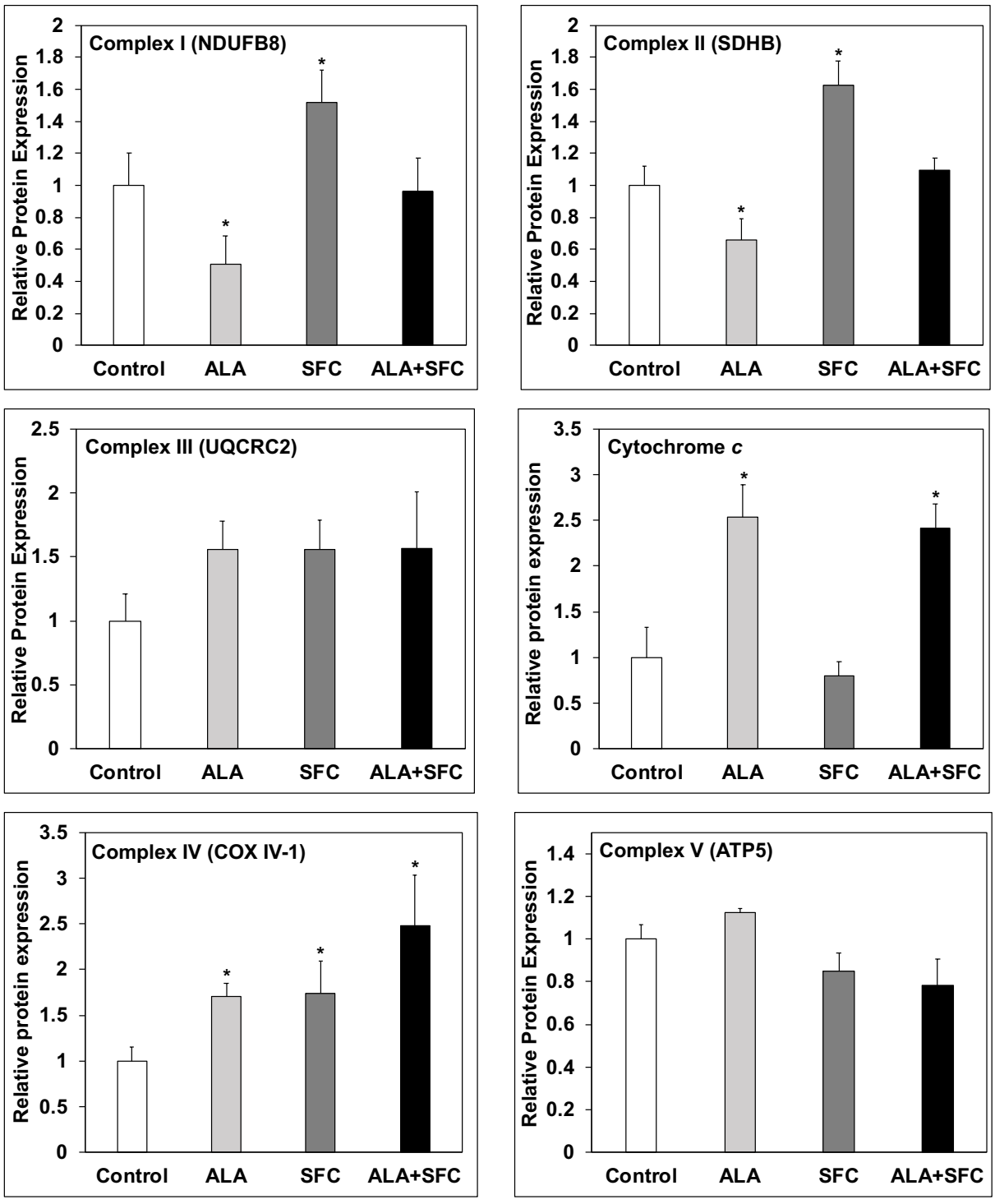

Figure 3.4 Protein levels of mitochondrial OXPHOS. (**A**) The protein expression levels of mitochondrial OXPHOS were measured by Western blot. (**B)** Graphs of band intensity ratio analysis relative to β-actin are shown. One-way ANOVA (Tukey's test) was performed for each data set to show significant differences in mean values between treated and untreated samples, **P* < 0.05, ***P* < 0.01 vs. nontreated control group (Control). Data are expressed as means ± standard deviation (SD) in three independent experiments

3.3.4 Measurement of enzymatic activities of COX

COX is one of five proteins in mitochondrial OXPHOS, which regulates the mitochondrial OXPHOS system (Sugiyama *et. al.,* 2012) ALA has been reported to increase COX activity in C57BL/6N mice (Ogura *et. al.,* 2011). To further study this effect, mitochondrial fractions extracted from ALA, SFC, and ALA+SFC administered myoblast cells were used to measure COX activity. COX activity was measured by quantifying the oxidation of reduced cytochrome *c*. COX activity obviously increased in the presence of ALA, SFC, and ALA+SFC (**Figure 3.5**; P < 0.01). This result indicates increased mitochondrial OXPHOS system capacity, suggesting increased mitochondrial activity.

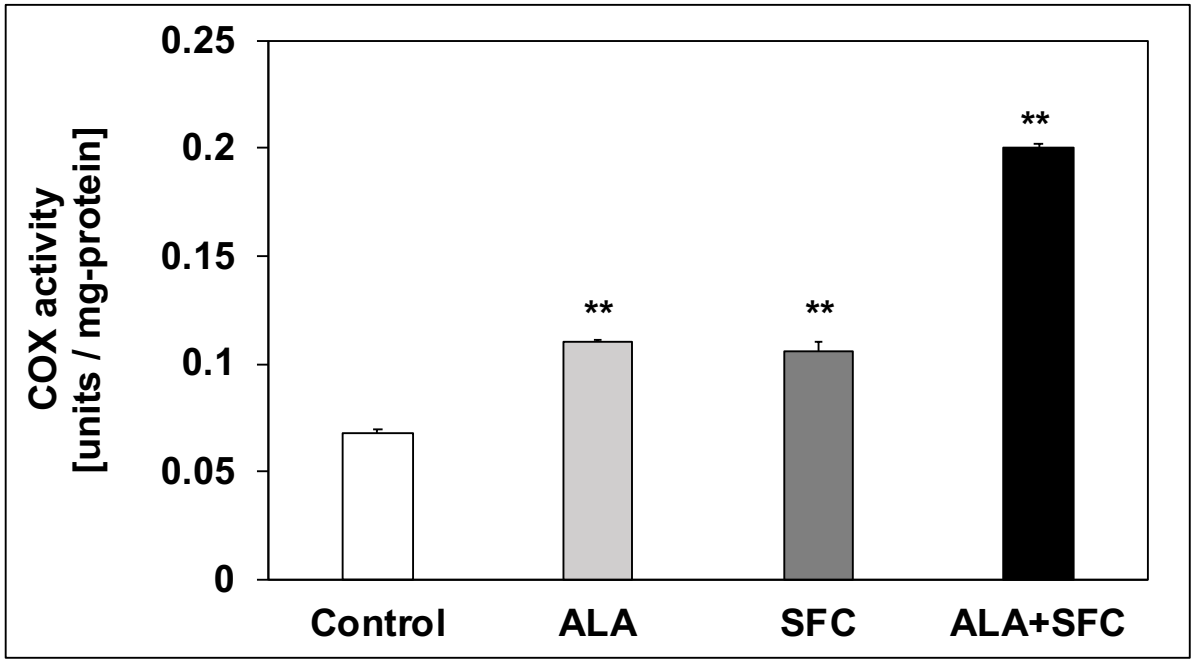

Figure 3.5 Enzymatic activity of COX per mg protein. COX activity was enhanced by ALA, SFC, and ALA+SFC. One-way ANOVA (Tukey's test) was performed for each data set to show significant differences in mean values between treated and untreated samples, **P* < 0.05, ***P* < 0.01 vs. nontreated control group (Control). Data are expressed as means ± standard deviation (SD) in three independent experiments

3.3.5 Determination of ATP production levels

ALA, SFC, and ALA+SFC were added to the myoblast cells to confirm this further. Mitochondrial fractions were extracted from each treatment (ALA, SFC, and ALA+SFC) to measure the ATP production levels. Supporting the occurrence of an increase in COX activity, ATP production levels are strongly promoted after treatment with ALA or SFC (**Figure 3.6**; *P* < 0.05) and more significant in ALA+SFC (**Figure 3.6;**

$P < 0.01$). These data show that ALA and SFC increased mitochondrial activity by activating COX activity by stimulating the mitochondrial OXPHOS system.

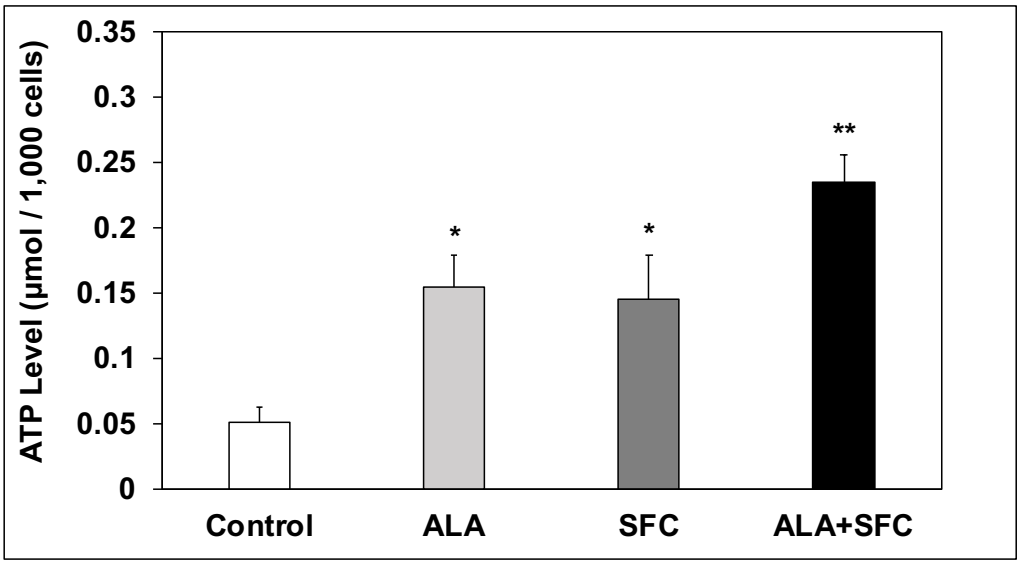

Figure 3.6. ATP production levels. ATP levels were promoted by adding ALA, SFC, and ALA+SFC. One-way ANOVA (Tukey's test) was performed for each data set to show significant differences in mean values between treated and untreated samples, $*P < 0.05$, $**P < 0.01$ vs. nontreated control group (Control). Data are expressed as means ± standard deviation (SD) in three independent experiments

3.3.6 Expression levels of the protein containing Fe-S clusters in mitochondria

In the aerobic growth of cells, iron-sulfur clusters have significant roles, including regulating enzyme activity and gene expression (Staples *et. al.,* 1996). Previously**,** **Figure 3.4** revealed that ALA significantly down-regulated the protein expression levels of mitochondrial OXPHOS complex I and complex II. Complex I and complex II containing iron-sulfur clusters, and the formation of these clusters requires free ion iron. Therefore, the decline of protein expression in both complexes was assumed because the formation of iron-sulfur clusters is disrupted by a lack of free ions in mitochondria. This phenomenon is caused by the increase in heme biosynthesis by the adding ALA that requires a tremendous amount of free iron. Therefore, the other proteins containing iron-sulfur clusters in mitochondria ferrochelatase (FECH) and aconitase 2 were analyzed; besides ALA, SFC was added as the free iron ion source. Protein expression levels of FECH and aconitase 2 are independent of mitochondrial OXPHOS, and both complexes were evaluated by Western blot (**Figure 3.7** (**A**)). Band intensity graphs were plotted in **Figure 3.7** (**B**). Expression levels of aconitase 2 and

FECH were significantly down-regulated following the addition of ALA (**Figure 3.7** (**B**); $P < 0.01$) and (**Figure 3.7** (**B**); $P < 0.05$), respectively; on the contrary, administration of SFC showed a significant upregulation in both proteins (**Figure 3.7** (**B**); $P < 0.05$). Besides, SFC reverses the reduction of protein expression of aconitase 2 and FECH caused by ALA addition back to the control level. Therefore, this evidence demonstrated that proteins containing iron-sulfur clusters are sensitive to the changes of free ion iron in mitochondria.

(A)

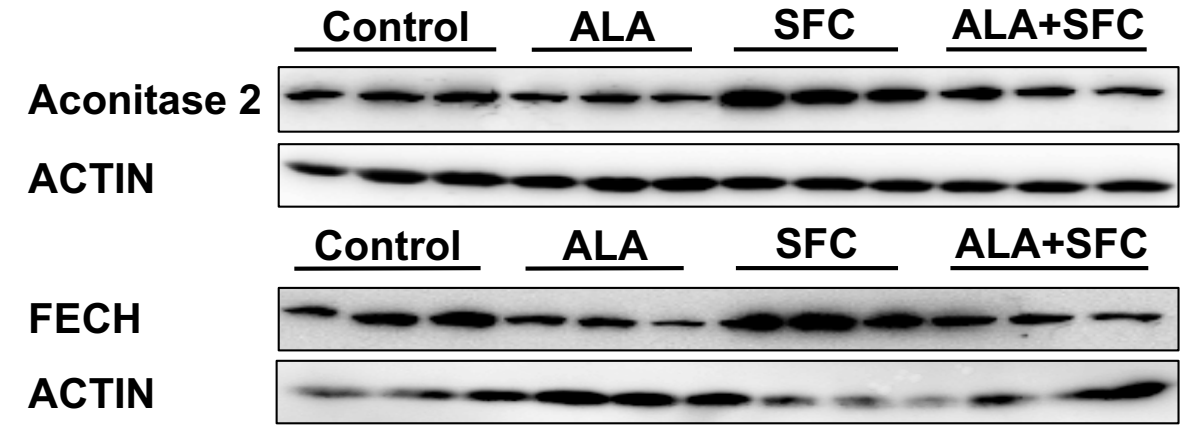

(B)

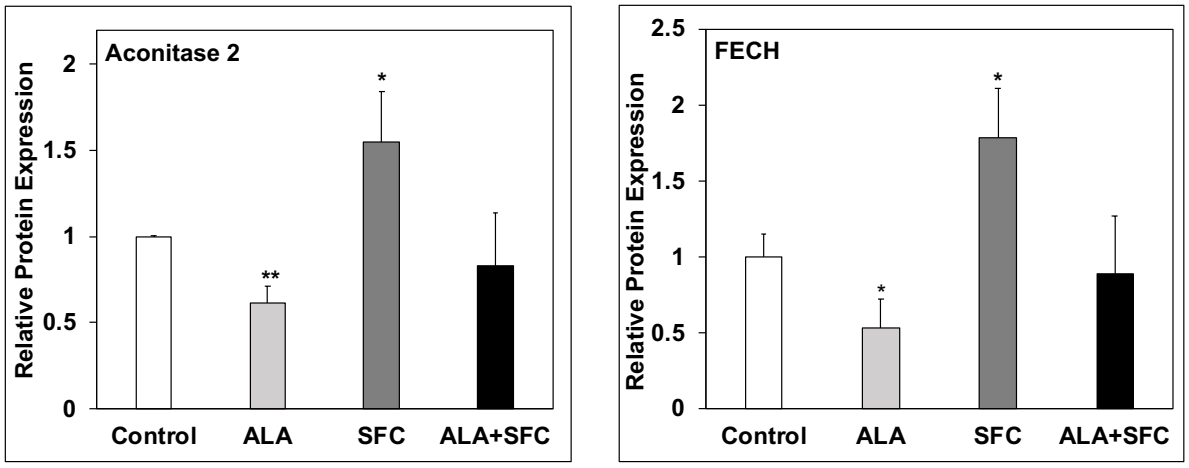

Figure 3.7 Protein levels of proteins containing iron-sulfur-clusters in mitochondria. (**A**) Expression levels of proteins that have the iron-sulfur clusters were measured by Western blot. (**B**) Graphs of band intensity ratio analysis relative to β-actin are shown. ALA down-regulated the protein expression levels of aconitase 2 and FECH. On the one hand, it was significantly increased by SFC, and it recovered back to the control level in ALA+SFC. One-way ANOVA (Tukey's test) was performed for each data set to show significant differences in mean values between treated and untreated samples, *P < 0.05, **P < 0,01 vs. nontreated control group (Control). Data are expressed as means ± standard deviation (SD) in three independent experiments.

3.4 DISCUSSION

Mitochondria have been recognized as the powerhouse of cells. It is the primary site to produce ATP in cells through the OXPHOS system and carries various metabolic functions. These include a central hub for multiple transducing in immune response and maintaining the heme homeostatis (Leighton et. al., 1995; Mehta et. al., 2017). Dysfunction in mitochondrial activities has been notorious as the cause of a variety of human disorders, such as aging, diabetes, cancer, and neurodegenerative diseases (Wallace, 1999; Stöckl *et. al.,* 2006). Consequently, maintaining mitochondrial activity is very important to prevent those diseases.

One of the functions of mitochondria is to regulate the heme homeostatis. Heme has a diverse biological function in cells, including electron transfer in the electron transport chain of the OXPHOS system (Lill *et. al.,* 2015). Moreover, changes in heme concentration directly impact heme proteins and mitochondrial activity. This study revealed the importance of heme precursor ALA and SFC as the source of free iron ions on mitochondrial activity in myoblast (C2C12) cells. This research has shown that ALA or SFC alone and a combination of ALA and SFC significantly enhanced heme production. These results correspond to several previous studies that showed that ALA stimulates the PpIX biosynthesis. Also, SFC is a source of free iron and induces ferrochelatase (Miura et. al., 2015). Accordingly, these data suggest that ALA and SFC are necessary to generate heme. To the best of our knowledge, this is the first study to investigate the effects of ALA and SFC on myoblast cells.

HO-1 degraded heme into iron, CO, and biliverdin. Furthermore, HO-1 and heme concentration in mitochondria is inseparable. This research demonstrated that HO-1 protein expression levels were significantly up-regulated in the addition of ALA or SFC alone. Moreover, these effects were further enhanced in the combination of ALA+SFC. The protein expression levels of HO-1 had the same trend as intracellular heme in the presence of ALA and SFC. Based on these outcomes, intracellular heme concentration and the expression levels of HO-1 have a consistent linear relationship.

The addition of ALA and ALA+SFC resulted in a significant increase of heme proteins in mitochondrial OXPHOS, such as cytochrome *c* and complex IV, where SFC only increased the complex IV. This phenomenon is supported by the fact that both ALA and SFC significantly increased intracellular heme. These data suggest that ALA and SFC trigger the activation of OXPHOS. Conversely, complex III and complex

V protein expression levels were most likely not affected by ALA, SFC, and ALA+SFC. On the other hand, ALA markedly reduced complex I and complex II protein expression levels. However, in the abundance of free iron ions by SFC addition, complex I and complex II significantly up-regulated. Then, the addition of ALA+SFC reversed the effect of ALA and recovered the protein expression levels of complex I and complex II back to the control level.

Further investigation revealed the decrease of complex I and complex II protein expression levels because both possess the iron-sulfur clusters that are sensitive to the changes of free ion iron in mitochondria. Iron-sulfur clusters are a versatile chemical utilized in prime life processes such as energy production, gene expression regulation, protein translation, and antiviral response (Fuss *et. al.,* 2015) Moreover, protein contains iron-sulfur clusters strongly associated with mitochondria, especially electron transfer in the electron transport chain (Johnson *et. al.*, 2005).

In mitochondria, free ion iron deficiency is caused by the tremendous amount of free iron ion required during the increased heme biosynthesis followed by the ALA administration. Similar results confirmed these findings on aconitase 2 and FECH protein expression levels in mitochondria. Both aconitase 2 and FECH have iron-sulfur clusters and are independent of the mitochondrial OXPHOS system but showed a similarity in profile with complex I and complex I in the presence of ALA and SFC. In addition, iron-sulfur clusters type [2Fe-2S] are present in complex I and complex II (Sheftel *et. al.,* 2010).

COX is the mitochondrial OXPHOS system enzyme that catalyzes the electron transfer from reduced cytochrome *c* to molecular oxygen (Flint *et. al.,* 1996); the electrons and hydrogen ions reduce molecular oxygen into water (Calhoun *et. al.,* 1994). In most mitochondrial disorders, COX activity was reported to be declined (Rak *et. al.,* 2016). Myoblast cells rely on mitochondrial OXPHOS to produce ATP (Chung *et. al.,* 2007; McMahon *et. al.,* 1994). In this study, it was observed that ALA, SFC, and ALA+SFC increased the activity of COX significantly. This finding is correlated with the up-regulation in the protein expression levels of heme protein after the addition of ALA, SFC, and ALA+SFC**,** except cytochrome *c* was not affected by the addition of SFC**.** Thus, these results illustrated that ALA, SFC, and ALA+SFC stimulate the OXPHOS system by increasing complex IV protein expression level and activity. In line with the increase of the OXPHOS system, the addition of ALA, SFC, and ALA+SFC effectively enhanced the ATP levels.

CHAPTER 4

5-AMINOLEVULINIC ACID AND SODIUM FERROUS CITRATE DECREASED CELL VIABILITY OF GASTRIC CANCER CELLS BY ENHANCED REACTIVE OXYGEN SPECIES GENERATION THROUGH IMPROVING CYTOCHROME *C* OXIDASE ACTIVITY

4.1 INTRODUCTION

Mitochondria have essential functions in cellular reactions, importantly in generation of energy in cells (Friedman *et. al.,* 2014; Brand *et. al.,* 2013). Mitochondria generate energy through OXPHOS system, it comprises five major membrane complexes and two-electron carriers in the inner mitochondrial membrane (Johnson *et. al.,* 1980). However, in cancer cells, there is a phenomenon, namely the Warburg effect, where cancer cells preferentially metabolize glucose by glycolysis in cytosol, producing lactate as an end product, despite the presence of oxygen (Gogvadze *et. al.,* 2010). In a recent study, deprivation of COX leads to mitochondrial disorders, such as cancer. Therefore, improving COX activity can shift this phenomenon to the usual citric acid cycle and OXPHOS in the mitochondria. Furthermore, COX activity can generate reactive oxygen species (ROS) (Hüttemann *et. al.,* 2012). Eventually, it can be an approach to killing the cancer cell.

5-aminolevulinic acid (ALA) is used widely used for photodynamic therapy (PDT). In this PDT, protoporphyrin IX (PpIX), which is converted from ALA (Paul *et. al*., 2017; Casas *et. al.,* 2001; Lai *et. al.,* 2019), can generate reactive oxygen species (ROS) that kill the cancer cell. ALA is also reported to promote cytochrome *c* oxidase (COX) activity, which can generate ROS (Peng *et. al.,* 1997). This study focused on the effect of ALA during PDT. In addition, in the previous study, sodium ferrous citrate (SFC) is reported to increase COX activity (Nishio et. al., 2014).

Previous studies have also reported that ALA increases heme biosynthesis (Miura *et. al.,* 2015), possibly increasing heme protein. Furthermore, mitochondrial respiration chain complex IV and cytochrome *c* are heme proteins. Moreover, ALA combined with SFC was reported to increase heme oxygenase-1 (HO-1) (Ito *et. al.,* 2018) However, in the previous studies, treatment in human gastric cancer cell line MKN45 has never targeted the COX activity that can generate ROS to reduce the cell viability with the combination of ALA and SFC (Yoshimoto *et. al.,* 2015). Therefore, this study focused on the effect of ALA during PDT. In addition, it also aims to investigate the ROS generation that kills the cancer cell with ALA and SFC as illustrated in **Figure 4.1** and its contribution to the effect of PDT.

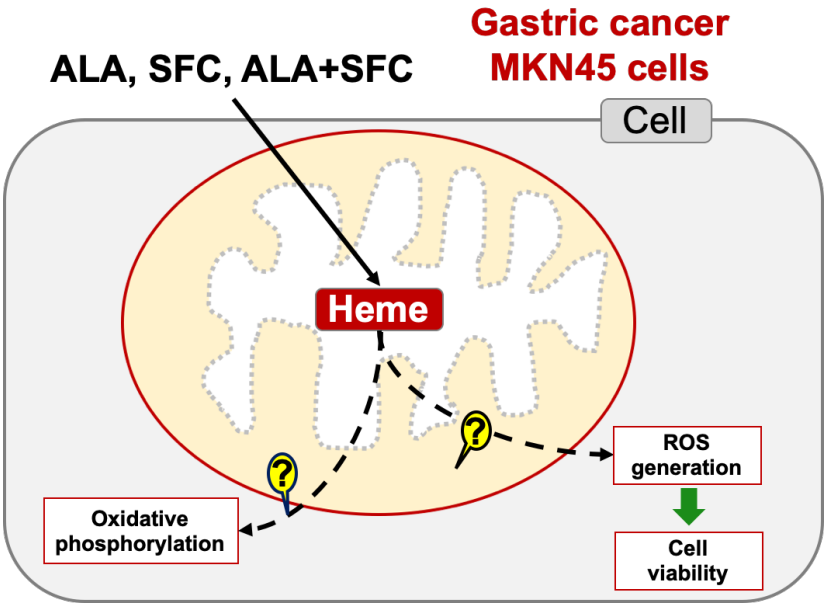

Figure 4.1 Conceptual diagram of addition of exogenous ALA, SFC, and ALA+SFC

4.2 MATERIALS & METHODS

Chemicals

ALA hydrochloride was purchased from Cosmo Bio Co., Ltd. (Tokyo, Japan). Sodium ferrous citrate (SFC) was purchased from Komatsuya Corporation (Osaka, Japan). Roswell Park Memorial Institute medium (RPMI) medium and antibiotic-antimycotic (ABAM) mixed-stock medium were purchased from Nacalai Tesque (Kyoto, Japan). Fetal bovine serum (FBS) was purchased from Equitech-Bi (Texas, USA).

Cell culture

Table 4.1 Amount of cell seeded for each experiment

Experiments	Seeding cell number (cells / well)
Heme production level	0.5 x 10^6 cells
HO-1 protein expression level	
Heme proteins expression level	
Intracellular ROS	
Cell viability	
COX activity measurement	0.5 x 10^7 cells

The human gastric cancer cell line MKN45 was obtained from Riken (Saitama, Japan). Cells were cultured and grew in growth medium (GM), GM [RPMI, D–(+)–glucose, L-glutamine, 10% FBS, and 10% ABAM] at 37°C in a 5% CO_2 incubator. For heme quantification, western blot, cell viability assay, and ROS measurement, (0.3×10^6 cells/mL) cells were seeded, while (5.0×10^6 cells/mL) cells were seeded for COX activity assay. Cells were treated with ALA (1 mM), SFC (0.05 mM), and ALA+SFC (1 mM+0.05 mM) for 96 hours, except for ROS measurement only for 24 hours under dark conditions considering the instability of SFC in light in all experiments. Cell number for seeding in various experiments is tabulated in **Table 4.1**.

Quantification of intracellular heme

Samples were lysed using NaOH, then cell suspensions were added into a mixture solution [1:9; (1 M CH_3COONH_3, 12.5% acetonitrile, pH 5.2):(50 mM CH_3COONH_3, 80% acetonitrile, pH 5.2)]. Heme concentration was measured by HPLC using the Type Prominence System from Shimadzu Corporation (Kyoto, Japan). The protein concentration of each sample was determined by Bradford's method using Quickstart Bradford 1x dye reagent from Biorad laboratories, Inc. (California, USA).

Enzymatic activities of cytochrome *c* oxidase

Measurement of COX activity was carried out by colorimetric analysis using cytochrome *c* oxidase kit (Sigma Aldrich Corporation, Tokyo, Japan). Protein concentration of the extracted mitochondria was determined by the Bradford method. Then, mitochondrial fractions were diluted and adjusted to 100 µg protein / 100 µl with enzyme dilution buffer containing 1 mM n-dodecyl β-D-maltoside. Reduced cytochrome *c* that reduced by dithiothreitol (DTT) was added to the sample and COX enzymatic activity was measured by following the oxidation of reduced cytochrome *c* at 550 nm. Cytochrome *c* has a large difference in molar absorptivity at 550 nm between the reduced and oxidized forms (Bery *et. al.,* 1987). Accordingly, the COX activity was calculated based on the absorbance of the oxidation of reduced cytochrome *c* at pH 7.0 and 25°C. Then, the rate of the oxidation of reduced cytochrome *c* (1.0 µmol / min) was defined as a unit.

Western blotting

Western blotting experiments were carried out to quantify the expression level of proteins in cell using modified method (Kogot-Levin *et. al.* 2016). Cells were first washed with PBS (-), followed by addition Lysis Buffer A [50 mM Tris-HCl (pH 7.4), 20 mM N-methylaleimide, 1 mM DTT, 1% (v/v) Triton X-100 and Protease inhibitor cocktail (Nacalai Tesque)]. The cell suspensions were homogenized using a 27 G syringe for at least 10 times and centrifuge at 1000 x *g* for 10 minutes at 4°C. Protein samples were then recovered and stored at -80°C freezer for future use.

Protein samples were next treated with SDS-PAGE electrophoresis using 7.5% and 11.25 polyacrylamide gel. These separated proteins were then transferred onto an Immobilon-P PVDF membrane (Milipore Corp., M.A) whereby blocking and antibody treatment would be carried out next. Blocking was carried out by incubating the membrane at room temperature for 60 minutes in 5% (w/v) skimmed milk dissolved in TBST [20 mM Tris-HCl (pH 7.4), 150 mM NaCl, 0.05% (v/v) Tween 20].

Mouse anti-cytochrome *c* oxidase sub unit I antibody (complex IV) (Santa Cruz Biotechnology Inc., Dallas, Texas, USA; 1:200 dilution), and human anti-actin antibody (MP Biomedicals, Santa Ana, CA, USA; 1:200 dilution) which served as internal control, were used in primary antibody treatment. Secondary antibody used in this study were horseradish peroxidase (HRP)-conjugated anti-mouse (Cell Signaling Technology, Beverly, MA, USA) and anti-rabbit IgG (Santa Cruz Biotechnology Inc., Dallas, Texas, USA) concentrate, which were diluted 3000 times in TBST solution. Substrate for HRP used in this study were Western Lightning Chemiluminescent Reagent Plus, Western Lightning Chemiluminescent Reagent Pro (PerkinElmer Life and Analytical Sciences, Waltham, MA, USA), Western Blot Ultra-Sensitive HRP substrate (TaKaRa Bio, Inc., Shiga, Japan). Chemiluminescent were used to quantify protein expression levels using Lumino Imaging Analyzer LAS-4000 mini (GE Healthcare UK, Amersham Place, England).

Cytotoxicity assay

Cytotoxicity level of specific reagents that used in various purposes was carried out by colorimetric analysis using 3-[4,5-dimethylthiazol-2-yl]-2,5-diphenyl tetrazolium bromide (MTT). Cells were grown in 96 well microplates, a specific chemical was added and dilution series was made by shift each 100 µL to the right lane, after that

96 well microplates was incubated for 96 hours at 37°C in a 5% CO_2 incubator. A 10 µL mixed PBS and MTT was added in each well then incubated for 4 hours at 37°C in a 5% CO_2 incubator, 100 µL 10% SDS was added then incubated for another 24 hours. Absorbance were measured in 2 different wavelengths at 570 nm and 650 nm using Multiskan FC (Thermo Fischer, Massachusetts, USA). The obtained data was analyzed using Microsoft Excel program.

Cell viability measurement

Cell viability analysis was performed using an MTT assay. The MTT substrate is prepared in a physiologically balanced solution to cells cultured in 96-well plates at a concentration of (5 mg/ml) and incubated for 4 hours. Then, the same amount of 10% (w/v) sodium dodecyl sulfate (SDS) was added, and the cell was cultured overnight. The quantity of formazan, an MTT metabolite, was measured by recording changes in absorbance at a measurement wavelength of 570 nm and a reference wavelength of 630 nm using a multiskan FC absorption microplate reader from Thermo Fisher Scientific (California, USA).

Measurement of intracellular ROS

Cells were grown until confluent, then ALA, SFC, and ALA+SFC were added and incubated. After 24 h, cells were washed with PBS. Then, 10 µM 2',7'-dichlorodihydrofluorescin diacetate DCFH-DA in HBSS (+) was added and incubated for 30 minutes. Subsequently, DCFH-DA in HBSS was discarded and replaced with 500 µL HBSS (-). Fluorescent intensity was measured using an f-7000 Fluorescence spectrophotometer from Hitachi (Tokyo, Japan). The excitation was set at 480 nm, whereas the emission was set at 525 nm.

4.3 RESULTS

4.3.1 Intracellular heme production levels

ALA is the heme precursor of heme production. Furthermore, intracellular heme levels were measured. **Figure 4.2** shows that ALA and SFC increase intracellular heme significantly. Moreover, the escalation was more evident in ALA+SFC. To conclude, the addition of ALA increased intracellular heme levels. Alongside the

existence of ALA, SFC as a source of iron ions was further induced by heme biosynthesis.

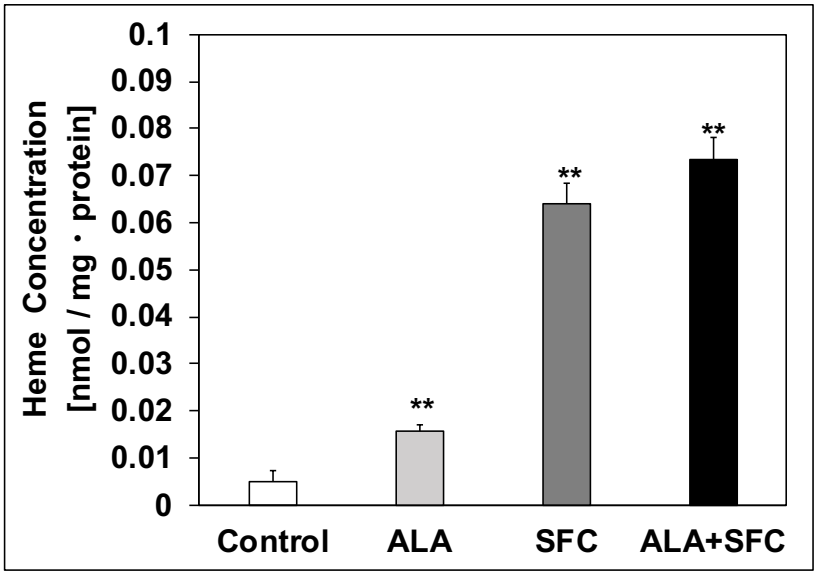

Figure 4.2 Intracellular heme concentration. Heme concentration was enhanced by ALA, SFC, and ALA+SFC. One-way ANOVA (Tukey's test) was performed for each data set to show significant differences in mean values between treated and untreated samples, *P < 0.05, **P < 0.01 vs. nontreated control group (Control). Data are expressed as means ± standard deviation (SD) in three independent experiments.

4.3.2 HO-1 protein expression levels

Western blot was performed to analyze the HO-1 protein expression level (**Figure 4.3** (**A**)). Band intensity ratio analysis from western blot results showed that HO-1 protein expression was elevated by the addition of ALA and SFC (**Figure 4.3** (**B**)). Thus, these results showed that the protein expression level of HO-1 is in line and consistent with the intracellular heme concentration.

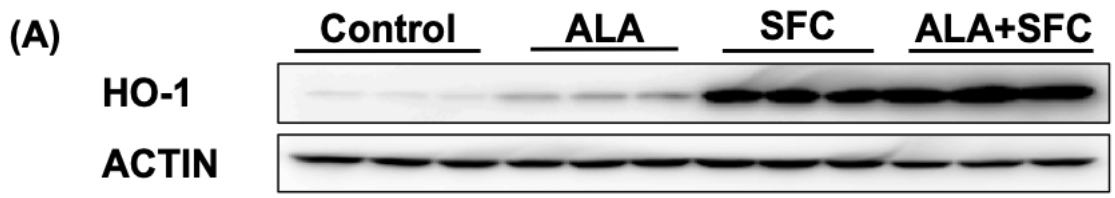

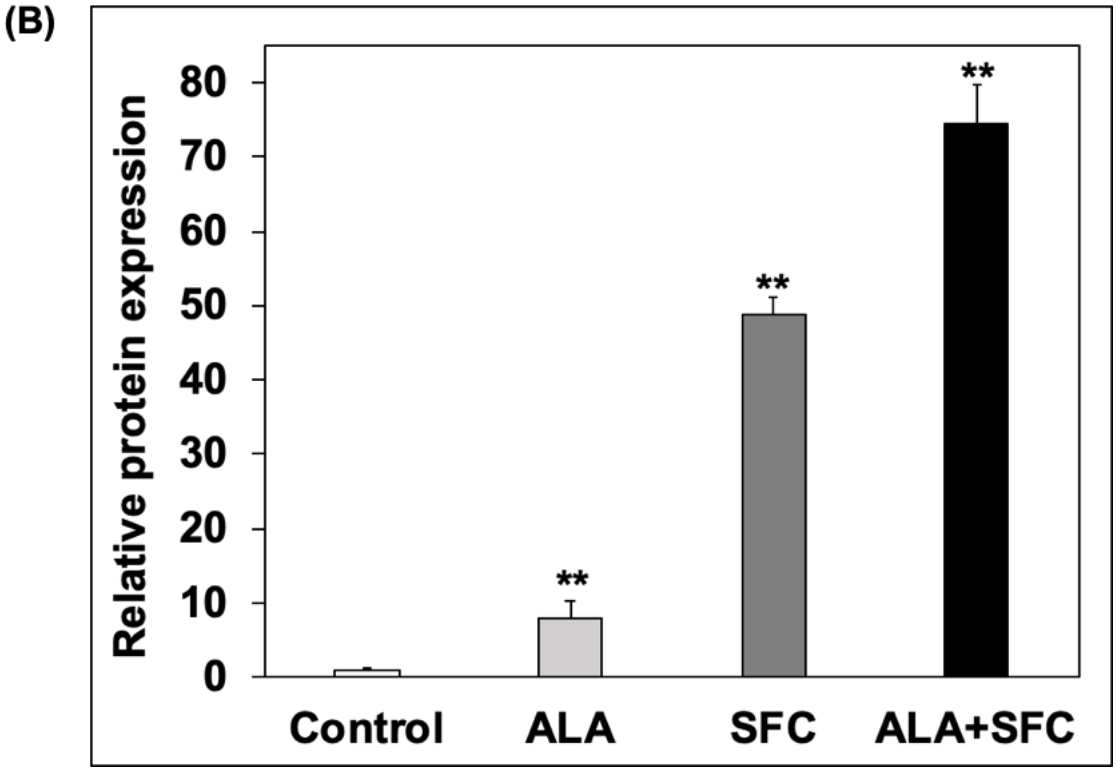

Figure 4.3 Protein levels of HO-1. (**A**) Western blot result of HO-1 protein. (**B**) Graphs of band intensity ratio analysis relative to β-actin are shown. HO-1 proteins were up-regulated by ALA, SFC, and ALA+SFC. One-way ANOVA (Tukey's test) was performed for each data set to show significant differences in mean values between treated and untreated samples, **P < 0.01 vs. nontreated control group (Control). Data are expressed as means ± standard deviation (SD) in three independent experiments.

4.3.3 Heme proteins expression levels

Heme is synthesized through the porphyrin pathway, in which ALA is the precursor. Then, ALA is converted into PpIX. Lastly, the insertion of ferrous ions produces heme, while SFC can provide the source of free iron ions. Heme functions as a protein-bound prosthetic group in mitochondrial OXPHOS complex IV and cytochrome *c*. A further effect of ALA on mitochondrial OXPHOS protein was studied by Western blot analyses (**Figure 4.4** (**A**)). The protein expression of cytochrome *c* and complex IV were significantly up-regulated following the administration of ALA, SFC, and ALA+SFC (**Figure 4.4** (**B**)). Taken together, hemeproteins in mitochondrial OXPHOS have shown a remarkable increase after the addition of ALA, SFC, and ALA+SFC.

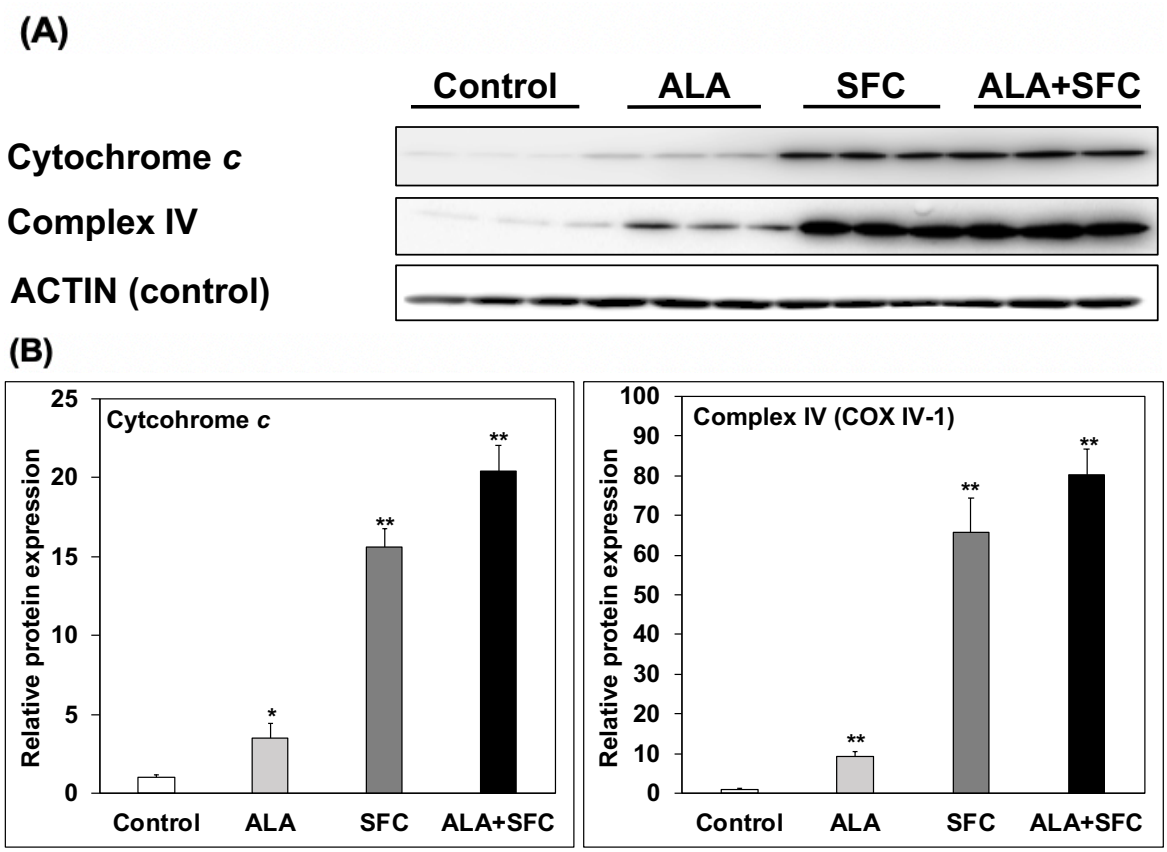

Figure 4.4 Protein levels of mitochondrial OXPHOS. (**A**) The protein expression levels of mitochondrial OXPHOS were measured by Western blot. (**B)** Graphs of band intensity ratio analysis relative to β-actin are shown. Cytochrome *c* and complex IV proteins were up-regulated by ALA, SFC and ALA+SFC. On the one hand, complex III and complex V were unaffected by ALA or SFC. One-way ANOVA (Tukey's test) was performed for each data set to show significant differences in mean values between treated and untreated samples, *P < 0.05 vs. nontreated control group (Control). Data are expressed as means ± standard deviation (SD) in three independent experiments.

4.3.4 COX activity measurement

COX is one of five proteins in mitochondrial OXPHOS, which regulates the mitochondrial OXPHOS system (Brunori *et. al.,* 1995). Mitochondrial fractions extracted from ALA, SFC, and ALA+SFC administered human gastric cancer cell line MKN45 were used to measure COX activity. COX activity was measured by quantifying the oxidation of reduced cytochrome *c*. COX activity significantly increased in the presence of ALA, SFC, and ALA+SFC, as shown in **Figure 4.5**. COX, as previously mentioned, can generate ROS. This result suggests an increasing generation of ROS itself.

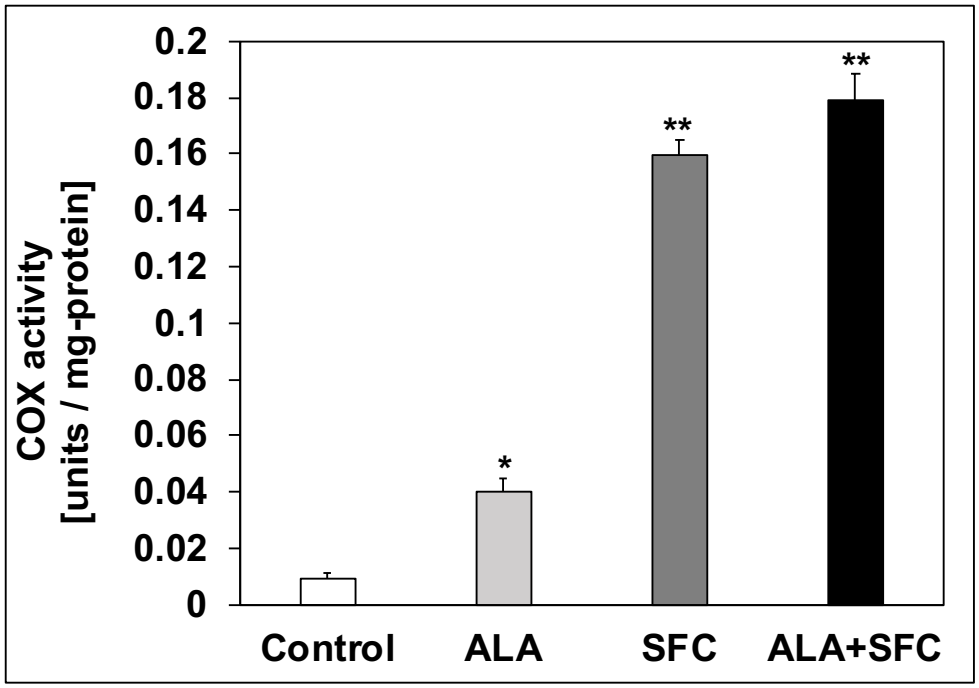

Figure 4.5 Enzymatic activity of COX per mg protein. COX activity was enhanced by ALA, SFC, and ALA+SFC. One-way ANOVA (Tukey's test) was performed for each data set to show significant differences in mean values between treated and untreated samples, **P < 0.01 vs. nontreated control group (Control). Data are expressed as means ± standard deviation (SD) in three independent experiments.

.

4.3.5 Intracellular ROS

DCFH-DA probe was used to measure intracellular ROS in human gastric cancer cell line MKN45 following the administration of ALA, SFC, and ALA+SFC. When using this probe, 2',7'-dichlorodihydrofluorescein (DCF) fluorescence is positively correlated with levels of ROS; thus, fluorescence intensity is considered proportional to the amount of intracellular ROS. In **Figure 4.6** relative fluorescent intensity showed enhanced fluorescence with the addition of ALA, SFC, and ALA+SFC.

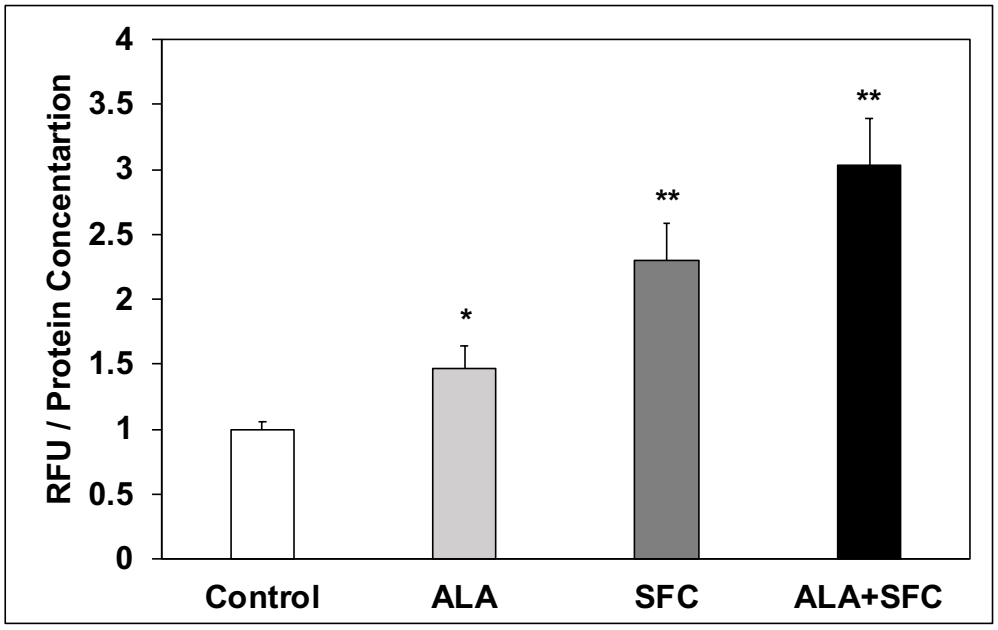

Figure 4.6 Cellular ROS levels. ROS was measured after the administration of ALA, SFC, and ALA+SFC after 24 hours of treatment. One-way ANOVA (Tukey's test) was performed for each data set to show significant differences in mean values between treated and untreated samples, *P < 0.05, **P < 0.01 vs. nontreated control group (Control). Data are means ± standard deviation (SD) of results in three independent experiments.

4.3.6 Cell viability

The viability of autologous cells is closely related to human health. Therefore, monitoring cell viability is vital for human health, sub-health, and disease detection (Zhang *et. al.,* 2020; Teodoro *et. al.,* 2012). In particular, cell viability monitoring also plays an essential role in drug screening, including drug development and efficacy evaluation (Ramirez *et. al.,* 2010). The standard method commonly used for detecting cell viability is the MTT assay (Kumar *et. al.,* 2018). Due to reduction by mitochondrial reductase, MTT with yellow color will turn into formazan with deep purple color. Cell viability assessed in the MTT assay after ALA, SFC, and ALA+SFC treatment is shown in **Figure 4.7**. Cell viability in human gastric cancer cell line MKN45 was significantly decreased in a concentration-dependent manner. This result corresponds to ALA that induced substantial intracellular ROS generation. Moreover, the combination of ALA+SFC generates more intracellular ROS.

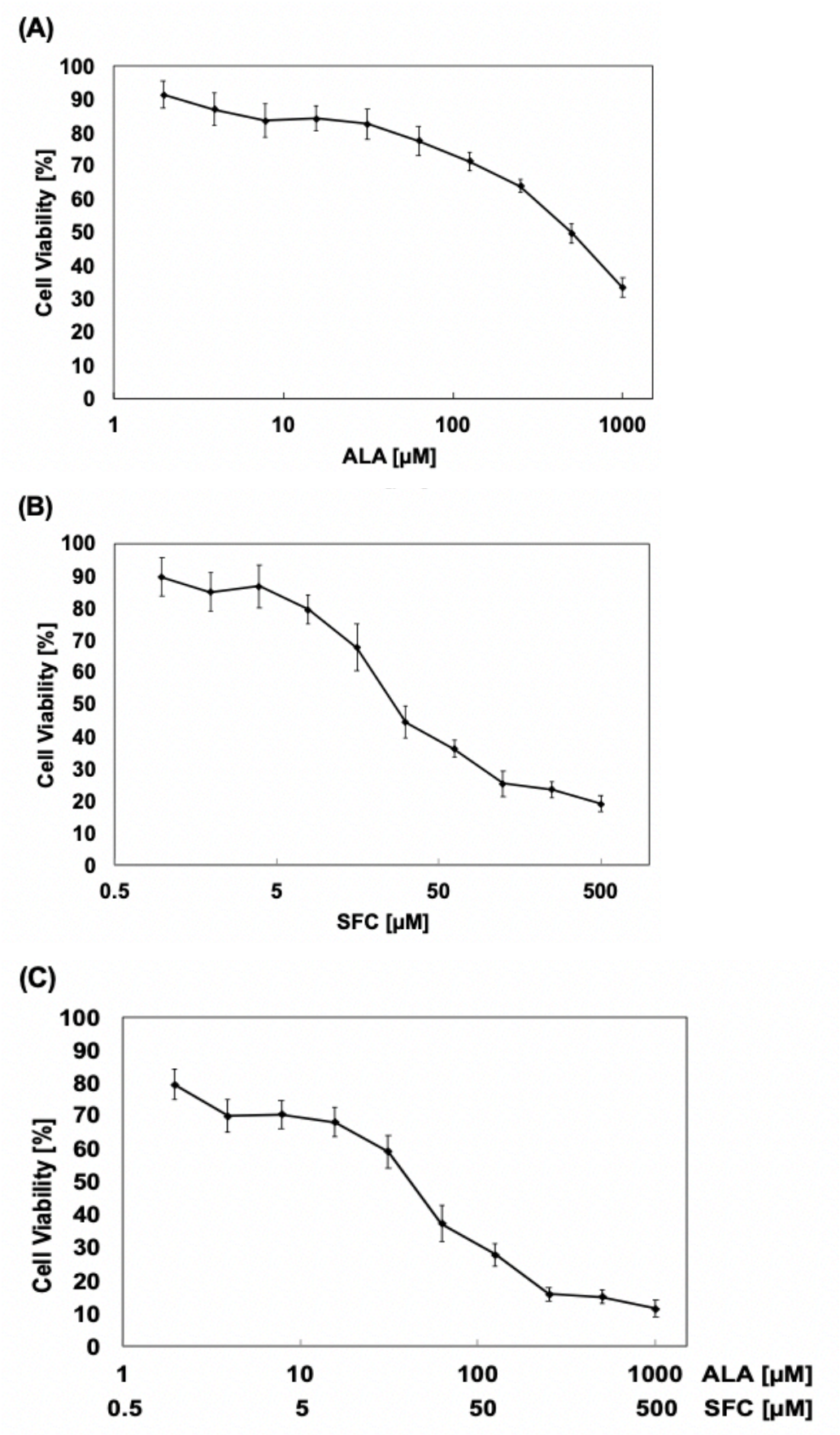

Figure 4.7. Cell. Viability. MTT assay was used ot evaluate the cell viability after the addition of (**A**) ALA, (**B**) SFC, and (**C**) ALA+SFC after 4 days of treatment.

4.4 Discussion

Mitochondria have been recognized as the powerhouse of cells. It produces energy through oxidative phosphorylation (OXPHOS) for cellular activities. Moreover, it is also maintaining the heme homeostatis (Chen *et. al.,* 2012; Krishnamurthy *et. al.,* 2007; Atamna *et. al.,* 2002). Furthermore, dysfunction in COX activity has been notorious as the cause of mitochondrial dysfunctions, including cancer (Fiorito *et. al.,* 2012; Perks *et. al.,* 2017; Rak *et. al.,* 2016). Heme has a diverse biological function in cells, including electron transfer in the electron transport chain of the OXPHOS system. This study revealed the combination of heme precursor ALA and SFC as the source of free iron ions increased the heme biosynthesis in mitochondria. Accordingly, these data suggest that ALA and SFC are essential to generate heme.

HO-1 degraded heme into iron, CO, and biliverdin. Furthermore, HO-1 and heme concentration in mitochondria is inseparable. This research demonstrated that HO-1 protein expression levels were significantly up-regulated in the presence of ALA and SFC. Based on these outcomes, intracellular heme concentration and the expression levels of HO-1 have a consistent linear relationship. Furthermore, the addition of ALA and SFC resulted in a significant increase of heme proteins of OXPHOS in mitochondria, namely cytochrome *c* and complex IV. This phenomenon suggests that ALA and SFC can trigger the activation of OXPHOS, including the COX activity.

COX is the last enzyme of the mitochondrial respiratory chain, and it is a regulation site for the mitochondria OXPHOS system (Kogot-Levin *et. al.,* 2016). It was observed that ALA and SFC increased the activity of COX significantly. This finding correlates with the up-regulation in the protein expression levels of heme protein after the addition of ALA and SFC. Thus, these results showed that ALA and SFC stimulate the OXPHOS system and COX activity. The increase in COX activity can reverse the Warburg effect. Consequently, it shifts back the preferentially metabolized glucose by glycolysis in the cytosol to generate energy in the cancer cell to the usual citric acid cycle and OXPHOS in the mitochondria. The increasing COX activity also causes electron leakage during the electron transport within the mitochondria.

Furthermore, the increased electron leakage during the electron transport in mitochondria causes excessive intracellular ROS production. It is proven that the addition of ALA and SFC effectively enhanced the generation of intracellular ROS. The occurrence of excessive ROS production cause cell death. This study shows that

cell viability decreases in a concentration-dependent manner following the addition of ALA and SFC.

In conclusion, ALA combined with SFC is proven to improve ROS generation, which causes rapid and substantial cytotoxic that reduces the cell viability of human gastric cancer cell line MKN45. Together, this study can detect ROS generation with ALA and SFC. Furthermore, this generation of ROS that has cytotoxic can contribute to the efficacy of PDT.

CHAPTER 5

SUMMARY

5.1 CONCLUSION

5.2 FUTURE CONSIDERATIONS

5.1 CONCLUSION

Mitochondria is the organelle that perform aerobic respiration and produce energy (ATP) through oxidative phosphorylation system which necessary for cellular activities (Bertram *et. al.,* 2006). It also plays an important role in controlling/signaling calcium (Ca^{2+}) which is essential for maintaining homeostasis of eukaryotic cells (Schatz, 1995). However, it has been found that the number and functions of mitochondria decrease in the process of aging and disease, then led to an abnormality in mitochondria. It is becoming very clear that the progress will be adversely affected, so improving the mitochondrial function and number are needed to eliminate the negative cycle due to mitochondrial abnormalities.

In the previous study, it has been investigated the differences of iron metabolism in tumor cells and in normal cells and found that the amount of mitochondrial labile iron ion in cancer cells was lower than that in normal cells (Hayasi *et. al.,* 2015). In addition, COX activity has been reported to decline in mitochondrial dysfunction, including in cancer cells (Rak *et. al.,* 2016). Therefore, in the present study, SFC was added for the free iron ions source, and the effect of ALA and SFC on cancer cells was analyzed.

This study has purpose to investigate the effect of ALA and SFC on mitochondrial activity in myoblast (C2C12) cells. Additionally, in cancer cells, this study also focused on the effect of ALA during PDT. Moreover, in the previous study, SFC is reported to increase COX activity. So, this study also aims to improve the COX activity by the addition of SFC that can promote ROS generation, which has a cytotoxic effect.

In summary, the findings in this study can be concluded as follows:

- The addition of ALA stimulates oxidative phosphorylation by upregulation COX in myoblast cells.
- The presence of ALA did not affect the mitochondrial content and mitochondrial biogenesis in myoblast cells.
- Mitochondrial activities were significantly improved by the addition of ALA in myoblast cells.
- The addition of ALA, SFC and ALA+SFC stimulates oxidative phosphorylation by upregulation of COX in myoblast cells.
- ALA markedly reduced the expression levels of the protein-containing Fe-S cluster. However, the abundance of free iron ions by SFC addition significantly

up-regulated the expression levels of protein-containing Fe-S cluster in myoblast cells.

- The addition of ALA, SFC, and ALA+SFC stimulates oxidative phosphorylation by upregulation COX in cancer cells.
- ALA, SFC, and ALA+SFC markedly reduced the cell viability in cancer cells by increasing ROS production.

In this study, it demonstrated that the addition of ALA as the heme precursor, SFC as an iron source, and the combination of ALA+SFC successfully increase heme production and contribute to the upregulation of heme proteins, resulting in the increase of COX activity and an increase in ATP levels in myoblast (C2C12) cells. Furthermore, the result showed that the addition of ALA, SFC, and the combination of ALA+SFC increased COX activity that shifts back the preferentially metabolized glucose by glycolysis in the cytosol to generate energy in the cancer cell to the usual citric acid cycle and OXPHOS in the mitochondria.

COX activity increases in both myoblast cells and cancer cells. Basal COX activity is higher in myoblast cells compared to in cancer cells 0.06 and 0.01 [units / mg-protein] consecutively. Then, with the addition of ALA, COX activity significantly increases in both cells 0.12 and 0.04 [units / mg-protein] consecutively. The administration of SFC also significantly increases the COX activity in both cells 0.11 and 0.16 [units / mg-protein] consecutively. Moreover, the combination of ALA+SFC obviously increase COX activity in both cells 0.21 and 0.18 [units / mg-protein] consecutively. Thus, the addition of ALA, SFC, and the combination ALA+SFC has more effective to increase the COX activity in myoblast cells compared to cancer cells.

The increasing of COX activity causes electron leakage during the electron transport within the mitochondria. Subsequently, excessive intracellular ROS production occurred, that leads to cell death. The basal level of COX activity is six times higher in myoblast compared to cancer cells. The ROS quenching system in myoblast is better compared to the cancer cells, even though ROS is produced in both cells. In cancer cells, the excessive amount of ROS that is accumulated that can cause the cell death. This phenomenon is not observed in myoblast cells.

In conclusion, this study demonstrated that ALA and SFC improve mitochondrial properties in myoblast (C2C12) cells. Furthermore, the same results were obtained in the cancer cells, which reduced their cell viability by increasing ROS production. In

conclusion, mitochondrial properties increase in myoblast, and this study also provides a novel treatment for mitochondrial dysfunction, especially cancer.

5.2 FUTURE CONSIDERATIONS

This research has successfully demonstrated that ALA and SFC are useful for improving mitochondrial activities through stimulating OXPHOS, which provides viable treatment options for mitochondrial diseases. Moreover, this study also can detect ROS generation with ALA and SFC. Furthermore, this generation of ROS has a cytotoxic effect. Therefore, this phenomenon contributes to the effect of PDT. However, further depth investigation should be considered, such as increasing the generation of ROS to maximize its contribution to the effect of PDT.

BIBLIOGRAPHY

Allen, J., Romay-Tallon, R., Brymer, K. J., Caruncho, H. J., & Kalynchuk, L. E. (2018). Mitochondria and mood: Mitochondrial dysfunction as a key player in the manifestation of depression. *Frontiers in Neuroscience*, 12(1), 1–13.

Atamna, H., Killilea, D. W., Killilea, A. N., & Ames, B. N. (2002). Heme deficiency may be a factor in the mitochondrial and neuronal decay of aging. *Proceedings of the National Academy of Sciences*, 99(23), 14807–14812.

Bertram, R., Gram Pedersen, M., Luciani, D. S., & Sherman, A. (2006). A simplified model for mitochondrial ATP production. *Journal of Theoretical Biology*, 243(4), 575–586.

Bery E. A., & Trumpoer B. L. (1987). Simultaneous determination of hemes a, b, and c from pyridine hemochrome spectra. *Anal Biochem*, 161(1),1–15.

Bhatti, J. S., Bhatti, G. K., & Reddy, P. H. (2018). Mitochondrial dysfunction and oxidative stress in metabolic disorders - A Step towards mitochondria based therapeutic strategies. *HHS Public Access*. *1863*(5), 1066–1077.

Bonawitz, N. D., Chatenay-Lapointe, M., Pan, Y., & Shadel, G. S. (2007). Reduced TOR Signaling Extends Chronological Life Span via Increased Respiration and Upregulation of Mitochondrial Gene Expression. *Cell Metabolism*, 5(4), 265–277.

Boushel, R., Gnaiger, E., Schjerling, P., Skovbro, M., Kraunsoe R & Dela F. (2007). Patients with type 2 diabetes have normal mitochondrial function in skeletal muscle. *Diabetologia*, 50, 790–796.

Brand, M. D., Orr, A. L., Perevoshchikova, I. V., & Quinlan, C. L. (2013). The role of mitochondrial function and cellular bioenergetics in ageing and disease. *British Journal of Dermatology*, 169(1), 1–8.

Brunori, M., & Wilson, M. T. (1995). Electron transfer and proton pumping in cytochrome oxidase. *Biochimie*, 77(8), 668–676.

Calhoun, M. W., Thomas, J. W., & Gennis, R. B. (1994). The cytochrome oxidase superfamily of redox-driven proton pumps. *Trends in Biochemical Sciences*, *19*(8), 325–330.

Candeias, E., Duarte, A. I., Carvalho, C., Correia, S. C., Cardoso, S., Santos, R. X., & Moreira, P. I. (2012). The impairment of insulin signaling in Alzheimer's disease. *IUBMB Life*, 64(12), 951–957.

Casas, A., Fukuda, H., Di Venosa, G., & Batlle, A. (2001). Photosensitization and mechanism of cytotoxicity induced by the use of ALA derivatives in photodynamic therapy. *British journal of cancer*, 85(2), 279–284.

Chen, C., & Paw, B. H. (2012). Cellular and mitochondrial iron homeostasis in vertebrates. *Biochimica et Biophysica Acta (BBA)-Molecular Cell Research*, 1823(9), 1459–1467.

Chrzanowska-Lightowlers, Z. M., Turnbull, D. M., & R.N. Lightowlers. (1993). A microtiter plate assay for cytochrome c oxidase in permeabilized whole cells. *Anal. Biochem*, 214:45–49.

Chung, S., Dzeja, P. P., Faustino, R. S., & Terzic, A. (2008). Developmental restructuring of the creatine kinase system integrates mitochondrial energetics with stem cell cardiogenesis. Annals of the New York Academy of Sciences 1147(1), 254–263

Chung, S., Dzeja, P. P., Faustino, R. S., Perez-Terzic, C., Behfar, A., & Terzic, A. (2007). Mitochondrial oxidative metabolism is required for the cardiac differentiation of stem cells. *Nature clinical practice Cardiovascular medicine*, 4(1), 60–67.

Coenen, M. J. H., Van Den Heuvel, L. P., Nijtmans, L. G. J., Morava, E., Marquardt, I., Girschick, H. J., & Smeitink, J. A. M. (1999). SURFEIT-1 gene analysis and two-dimensional blue native gel electrophoresis in cytochrome c oxidase deficiency. *Biochemical and Biophysical Research Communications*, *265*(2), 339–344.

Conley, K. E., Jubrias, S. A., & Esselman, P. C. (2000). Oxidative capacity and ageing in human muscle. *Journal of Physiology*, 526(1), 203–210.

Crofts, A. R. (2004). The Cytochrome bc_1 Complex: Function in the Context of Structure. *Annual Review of Physiology*, *66*(1), 689–733.

Desler, C., Marcker, M. L., Singh, K. K., & Rasmussen, L. J. (2011). The Importance of Mitochondrial DNA in Aging and Cancer. *Journal of Aging Research*, 2011, 1–9.

Di Lisa, F., & Bernardi, P. (1998). Mitochondrial function as a determinant of recovery or death in cell response to injury. *Molecular and Cellular Biochemistry*, 184: 379–391.

Dragon, S., Hille, R., Gotz, R., & Baumann, R. (1998). Adenosine 3′-5′-cyclic monophosphate (cAMP)-inducible pyrimidine 5′-nucleotidase and pyrimidine nucleotide metabolism of chick embryonic erythrocytes. *Blood*, 91:3052–8.

Fiorito, V., Chiabrando, D., & Tolosano, E. (2018). Mitochondrial targeting in neurodegeneration: a heme perspective. *Pharmaceuticals*, 11(3), 87–108.

Flint, D. H., & Allen, R. M. (1996). Iron− sulfur proteins with nonredox functions. *Chemical reviews*, *96*(7), 2315–2334.

Fortes, G. B., Alves, L. S., De Oliveira, R., Dutra, F. F., Rodrigues, D., Fernandez, P. L., & Bozza, M. T. (2012). Heme induces programmed necrosis on macrophages through autocrine TNF and ROS production. *Blood*, *119*(10), 2368–2375.

François, R., Jornayvaz, Gerald, I., & Shulman. (2014). Regulation of mitochondrial biogenesis. *Essays Biochem*, 47, 1–15.

Friedman, J. R., & Nunnari, J. (2014). Mitochondrial form and function. *Nature*, 505(7483), 335–343.

Fuss, J. O., Tsai, C. L., Ishida, J. P., & Tainer, J. A. (2015). Emerging critical roles of Fe–S clusters in DNA replication and repair. *Biochimica et Biophysica Acta (BBA)-Molecular Cell Research*, 1853(6), 1253–1271.

Gerbitz, K D., Gempel K., & Brdiczka. (1996). Mitochondria and diabetes. Genetic, biochemical, and clinical implications of the cellular energy circuit. *Diabetes*, 45(2), 113–126.

Ghezzi, D., & Zeviani, M. (2018). Human diseases associated with defects in assembly of OXPHOS complexes. *Essays In Biochemistry*, *62*(3), 271–286.

Gogvadze, V., Zhivotovsky, B., & Orrenius, S. (2010). The Warburg effect and mitochondrial stability in cancer cells. *Molecular aspects of medicine*, 31(1), 60–74.

Gribble, F. M., Loussouarn, G., Tucker, S. J., Zhao, C., Nichols, C. G., & Ashcroft, F. M. (2000). A novel method for measurement of submembrane ATP concentration. *J Biol Chem*, 275:30046–30049.

Gris, D. (2009). The role of mitochondria in health and disease. *Public Access NIH Public Access*, 9(6), 780–786.

Gris, D. (2013). The role of mitochondrial function and cellular bioenergetics in ageing and disease. *Public Access NIH Public Access*, 169(2), 1–8.

Hayashi, M., Fukuhara, H., Inoue, K., Shuin, T. & Ogura, S. I. (2015). The effect of iron ion on the specificity of photodynamic therapy with 5-aminolevulinic acid. *PLoS One*, 10(1), 1–11.

Hüttemann, M., Helling, S., Sanderson, T. H., Sinkler, C., Samavati, L., Mahapatra, G., & Lee, I. (2012). Regulation of mitochondrial respiration and apoptosis through cell signaling: cytochrome c oxidase and cytochrome c in ischemia/reperfusion injury and inflammation. *Biochimica et Biophysica Acta (BBA)-Bioenergetics*, 1817(4), 598–609.

Hüttemann, M., Lee, I., Pecinova, A., Pecina, P., Przyklenk, K., & Doan, J. W. (2008). Regulation of oxidative phosphorylation, the mitochondrial membrane potential, and their role in human disease. Journal of bioenergetics and biomembranes, 40(5), 445–456.

Hwang, A., Jeong, D. E., & Lee, S. J. (2012). Mitochondria and Organismal Longevity. *Current Genomics*, 13(7), 519–532.

I**to, H., Nishio, Y., Hara, T., Sugihara, H., Tanaka, T., & Li, X. K. (2018).** Oral administration of 5-aminolevulinic acid induces heme oxygenase-1 expression in peripheral blood mononuclear cells of healthy human subjects in combination with ferrous iron. *European Journal of Pharmacology*, 833(1), 25–33.

Johnson, D. C., Dean, D. R., Smith, A. D., & Johnson, M. K. (2005). Structure, function, and formation of biological iron-sulfur clusters. *Annual review of biochemistry*, 74(2), 226–237.

Johnson, L. V., Walsh, M. L., & Chen, L. B. (1980). Localization of mitochondria in living cells with rhodamine 123. *Proceedings of the National Academy of Sciences*, 77(2), 990–994.

Kawashima, S. (1991). Inhibition of rat liver transglutaminase by nucleotides. *Experientia*, 47:709–712.

Kogot-Levin, A., Saada, A., Leibowitz, G., Soiferman, D., Douiev, L., Raz, I., & Weksler-Zangen, S. (2016). Upregulation of mitochondrial content in cytochrome c oxidase deficient fibroblasts. *PLoS ONE*, 11(10), 1–18.

Komatsu, N., Arita, K., Mitsui, H., Nemoto, T., & Hanaki, K. (2021). Efficacy and safety of ferric citrate hydrate compared with sodium ferrous citrate in Japanese patients with iron deficiency anemia: a randomized, double-blind, phase 3 non-inferiority study. *International Journal of Hematology*, 114(1), 8–17.

Krammer, B., & Plaetzer, K. (2008). ALA and its clinical impact, from bench to bedside. *Photochemical and Photobiological Sciences*, *7*(3), 283–289.

Krishnamurthy, P., Xie, T., & Schuetz, J. D. (2007). The role of transporters in cellular heme and porphyrin homeostasis. *Pharmacology & therapeutics*, 114(3), 345–358.

Kumar, P., Nagarajan, A. & Uchil, P. D. (2018). Analysis of cell viability by the alamarblue assay. *Cold Spring Harbor Protocols*. 6(1), 469–73.

Lai, H. W., Sasaki, R., Usuki, S., Nakajima, M., Tanaka, T., & Ogura, S. I. (2019). Novel strategy to increase specificity of ALA-Induced PpIX accumulation through inhibition of transporters involved in ALA uptake. *Photodiagnosis and Photodynamic Therapy*, 27(1), 327–335.

Lane, N., & Martin, W. (2010). The energetics of genome complexity. *Nature*, 467(7318), 928–934.

Lange, C., & Hunte, C. (2002). Crystal structure of the yeast cytochrome bc1 complex with its bound substrate cytochrome c. *Proceedings of the National Academy of Sciences*, *99*(5), 2800–2805.

Larcombe-McDouall J, Buttell N, Harrison N, & Wray S. (1999). In vivo pH and metabolite changes during a single contraction in rat uterine smooth muscle. *J Physiol*, 518:783–790.

Larsen, S., Nielsen, J., Hansen, C. N., Nielsen, L. B., Wibrand, F., Stride, N., & Hey-Mogensen, M. (2012). Biomarkers of mitochondrial content in skeletal muscle of healthy young human subjects. *Journal of Physiology*, *590*(14), 3349–3360.

Layer, G., Reichelt, J., Jahn, D., & Heinz, D. W. (2010). Structure and function of enzymes in heme biosynthesis. *Protein Science*, *19*(6), 1137–1161.

Lebiedzinska, M., Karkucinska-Wieckowska, A., Wojtala, A., Suski, J. M., Szabadkai, G., Wilczynski, G., & Wieckowski, M. R. (2013). Disrupted ATP synthase activity and mitochondrial hyperpolarisation- dependent oxidative stress is associated with p66Shc phosphorylation in fibroblasts of NARP patients. *International Journal of Biochemistry and Cell Biology*, 45(1), 141–150.

Leighton, J., & Schatz, G. (1995). An ABC transporter in the mitochondrial inner membrane is required for normal growth of yeast. *The EMBO journal*, 14(1), 188–195.

Li, S., Takahara, T., Li, X. K., Fujino, M., Sugiyama, T., Tsukada, K., & Takahara, S. (2016). 5-Aminolevulinic acid combined with ferrous iron ameliorate ischemia–reperfusion injury in the mouse fatty liver model. *Biochemical and biophysical research communications*, 470(4), 900–906.

Lill, R., Dutkiewicz, R., Freibert, S. A., Heidenreich, T., Mascarenhas, J., Netz, D. J., & Mühlenhoff, U. (2015). The role of mitochondria and the CIA machinery in the maturation of cytosolic and nuclear iron–sulfur proteins. *European journal of cell biology*, 94(7-9), 280–291.

Manley, G. (2013). Structure, function, and assembly of heme centers in mitochondrial respiratory complexes. *Public Access NIH Public Access*. 71(2), 233–236.

McMahon, D. K., Anderson, P. A., Nassar, R. A. S. H. I. D., Bunting, J. B., Saba, Z., Oakeley, A. E., & Malouf, N. N. (1994). C2C12 cells: biophysical, biochemical, and immunocytochemical properties. *American Journal of Physiology-Cell Physiology*, 266(6), 1795–1802.

Mehta, M. M., Weinberg, S. E., & Chandel, N. S. (2017). Mitochondrial control of immunity: beyond ATP. *Nature Reviews Immunology*, 17(10), 608–620.

Mercer, T. R., Neph, S., Dinger, M. E., Crawford, J., Smith, M. A., Shearwood, A. M. J., & Mattick, J. S. (2011). The human mitochondrial transcriptome. *Cell*, 146(4), 645–658.

Mitchell, P. (1966). Chemiosmotic Coupling in Oxidative and Photosynhetic Phosphorylation ("First Book", 1966) - 1. *Bio. Rev.*, *41*, 445–502.

Miura, M., Ito, K., Hayashi, M., Nakajima, M., Tanaka, T., & Ogura, S. I. (2015). The effect of 5-aminolevulinic acid on cytochrome P450-mediated prodrug activation. *PLoS ONE*, *10*(7), 1–9.

Miyazaki, T., Neff, L., Tanaka, S., Horne, W. C., & Baron, R. (2003). Regulation of cytochrome c oxidase activity by c-Src in osteoclasts. *Journal of Cell Biology*, 160(5), 709–718.

Mizuno, Y., Ohta, S., Tanaka, M., Takamiya, S., Suzuki, K., Sato, T., & Kagawa, Y. (1989). Deficiencies in Complex I subunits of the respiratory chain in Parkinson's disease. *Biochemical and Biophysical Research Communications*, 163(3), 1450–1455.

Moghaddas, S., Hoppel, C. L., & Lesnefsky, E. J. (2003). Aging defect at the QO site of complex III augments oxyradical production in rat heart interfibrillar mitochondria. *Archives of Biochemistry and Biophysics*, 414(1), 59–66.

Muench, S. P., Trinick, J., & Harrison, M. A. (2011). Structural divergence of the rotary ATPases. In *Quarterly Reviews of Biophysics*. 44, (3), 311–356.

Nishio, Y., Fujino, M., Zhao, M., Ishii, T., Ishizuka, M., Ito, H., & Li, X. K. (2014). 5-Aminolevulinic acid combined with ferrous iron enhances the expression of heme oxygenase-1. *International immunopharmacology*, 19(2), 300–307.

Nunnari, J. & Jonathan, R.F. (2008). Mitochondrial form and function. *Nano*, *6*(9), 2166–2171.

Nunnari, J., & Suomalainen, A. (2012). Mitochondria: In Sickness and in Health. *Cell*, 148(6):1145–59.

Ogura, S. I., Maruyama, K., Hagiya, Y., Sugiyama, Y., Tsuchiya, K., Takahashi, K., & Tanaka, T. (2011). The effect of 5-aminolevulinic acid on cytochrome c oxidase activity in mouse liver. *BMC Research Notes*, 4(1), 2–5.

Ogura, S. I., Maruyama, K., Hagiya, Y., Sugiyama, Y., Tsuchiya, K., Takahashi, K., & Tanaka, T. (2011). The effect of 5-aminolevulinic acid on cytochrome c oxidase activity in mouse liver. *BMC research notes*, 4(1), 1–4.

Palmeira, C. M., & Rolo, A. P. (2004). Mitochondrially-mediated toxicity of bile acids. *Toxicology*, *203*(1–3), 1–15.

Paoli, M., Marles-Wright, J., & Smith, A. N. N. (2002). Structure–function relationships in heme-proteins. *DNA and cell biology*, 21(4), 271-280.

Paradies, G., Ruggiero, F. M., Petrosillo, G., & Quagliariello, E. (1993). Age-dependent decrease in the cytochrome c oxidase activity and changes in phospholipids in rat-heart mitochondria. *Archives of Gerontology and Geriatrics*, *16*(3), 263–272.

Parish, R., & Petersen, K. F. (2005). Mitochondrial dysfunction and type 2 diabetes. *Current Diabetes Reports*, 5(3), 177–183.

Patel, M. N. (2002). Oxidative stress, mitochondrial dysfunction, and epilepsy. *Free Radical Research*, 36(11), 1139–1146.

Paul, B. T., Manz, D. H., Torti, F. M., & Torti, S. V. (2017). Mitochondria and Iron: current questions. *Expert review of hematology*, 10(1), 65–79.

Payne, B. A. I., & Chinnery, P. F. (2015). Mitochondrial dysfunction in aging: Much progress but many unresolved questions. *Biochimica et Biophysica Acta - Bioenergetics*, 1847(11), 1347–1353.

Peng, Q., Warloe, T., Berg, K., Moan, J., Kongshaug, M., Giercksky, K. E., & Nesland, J. M. (1997). 5-Aminolevulinic acid-based photodynamic therapy:

clinical research and future challenges. *Cancer: Interdisciplinary International Journal of the American Cancer Society*, 79(12), 2282–2308.

Perks, K. L., Ferreira, N., Richman, T. R. & Filipovska. (2017). Adult-onset obesity is triggered by impaired mitochondrial gene expression. *Science Advances*. 3(8), 1–17.

Phielix E, Schrauwen-Hinderling V. B., Mensink M, Lenaers E, Meex R, Hoeks J, Kooi M. E., Moonen-Kornips E, Sels J. P., Hesselink, M. K., & Schrauwen, P. (2008). Lower intrinsic ADP-stimulated mitochondrial respiration underlies in vivo mitochondrial dysfunction in muscle of male type 2 diabetic patients. *Diabetes*, 57, 2943–2949

Quintela-Carvalho, G., Luz, N. F., Celes, F. S., Zanette, D. L., Andrade, D., Menezes, D., & Borges, V. M. (2017). Heme drives oxidative stress-associated cell death in human neutrophils infected with Leishmania infantum. *Frontiers in Immunology*, 8:1620.

Rak, M., Benit, P., Chretien, D., Bouchereau, J., Schiff, M., El-Khoury, R., & Rustin, P. (2016). Mitochondrial cytochrome c oxidase deficiency. *Clinical Science*, 130(6), 393–407.

Ramirez, C. N., Antczak, C., & Djaballah, H. (2010). Cell viability assessment: toward content-rich platforms. *Expert opinion on drug discovery*, 5(3), 223–233.

Reedy, C. J., & Gibney, B. R. (2004). Heme protein assemblies. *Chemical reviews*, 104(2), 617–650.

Ritov, V. B., Menshikova, E. V., He, J., Ferrell, R. E., Goodpaster, B. H., & Kelley, D. E. (2005). Deficiency of subsarcolemmal mitochondria in obesity and type 2 diabetes. *Diabetes*, 54(1), 8–14.

Saraste, M. (1999). Oxidative phosphorylation at the fin de siècle. *Science*, *283*(5407), 1488–1493.

Sazanov, L. A., & Hinchliffe, P. (2010). Structure of the Hydrophilic Domain. *Science*, 1430(2006), 1430–1436.

Scarpulla, R. C. (2006). Nuclear control of respiratory gene expression in mammalian cells. *Journal of Cellular Biochemistry*, 97(4), 673–683.

Schatz, G. (1995). An ABC transporter in the mitochondrial inner membrane is required for normal growth of yeast. *The EMBO Journal*, 14(1), 188–195.

Sheftel, A., Stehling, O., & Lill, R. (2010). Iron–sulfur proteins in health and disease. *Trends in Endocrinology & Metabolism*, 21(5), 302–314.

Sheng, B., Wang, X., Su, B., Lee, H. G., Casadesus, G., Perry, G., & Zhu, X. (2012). Impaired mitochondrial biogenesis contributes to mitochondrial dysfunction in Alzheimer's disease. *Journal of Neurochemistry*, 120(3), 419–429.

Shimizu, S. (2019). Organelle zones in mitochondria. *Journal of Biochemistry*, *165*(2), 101–107.

Shimura, M., Nozawa, N., Ogawa-Tominaga, M., Fushimi, T., Tajika, M., Ichimoto, K., & Murayama, K. (2019). Effects of 5-aminolevulinic acid and sodium ferrous citrate on fibroblasts from individuals with mitochondrial diseases. *Scientific reports*, 9(1), 1–11.

Short, K. R., Bigelow, M. L., Kahl, J., Singh, R., Coenen-Schimke, J., Raghavakaimal, S., & Nair, K. S. (2005). Decline in skeletal muscle mitochondrial function with aging in humans. *Proceedings of the National Academy of Sciences*, 102(15), 5618–5623.

Smith, L. D., & Garg, U. (2017). Urea cycle and other disorders of hyperammonemia. In Biomarkers in Inborn Errors of Metabolism. *Elsevier Inc*. 103–121.

Sohal, R. S. (1993). Aging, cytochrome c oxidase activity, and hydrogen peroxidase release by mitochondria. *Free radic Biol Med*. 14(6): 583–8.

Spinazzi, M., Casarin, A., Pertegato, V., Salviati, L., & Angelini, C. (2012). Assessment of mitochondrial respiratory chain enzymatic activities on tissues and cultured cells. *Nature Protocols*, 7(6), 1235–1246.

Srivastava, S. (2017). The mitochondrial basis of aging and age-related disorders. *Genes*, 8(12), 398.

Staples, C. R., Ameyibor, E., Fu, W., Gardet-Salvi, L., Stritt-Etter, A. L., Schürmann, P., & Johnson, M. K. (1996). The function and properties of the iron− sulfur center in spinach ferredoxin: thioredoxin reductase: a new biological role for iron− sulfur clusters. *Biochemistry*, 35(35), 11425–11434.

Stark, R., Guebre-Egziabher, F., Zhao, X., Feriod, C., Dong, J., Alves, T. C., & Kibbey, R. G. (2014). A role for mitochondrial phosphoenolpyruvate carboxykinase (PEPCK-M) in the regulation of hepatic gluconeogenesis. *Journal of Biological Chemistry*, 289(11), 7257–7263.

Stöckl, P., Hütter, E., Zwerschke, W., & Jansen-Dürr, P. (2006). Sustained inhibition of oxidative phosphorylation impairs cell proliferation and induces premature senescence in human fibroblasts. *Experimental Gerontology*, 41(7), 674–682.

Stummer, W., Pichlmeier, U., Meinel, T., Wiestler, O. D., Zanella, F., & Reulen, H. J. (2006). Fluorescence-guided surgery with 5-aminolevulinic acid for resection of malignant glioma: a randomised controlled multicentre phase III trial. *Lancet Oncology*, *7*(5), 392–401.

Sugiyama, Y., Hagiya, Y., & Hayashi T. (2012). The effect of 5-aminolevulinic acid on cytochrome c oxidase activity. *ALA-Porphyrin Science,* 1(1),17–21.

Sugiyama, Y., Hagiya, Y., Hayashi, T., & Ogura, S.I. (2012). The effect of 5-aminolevulinic acid on cytochrome *c* oxidase activity. *ALA-Porphyrin Science,* 1(1), 17–21.

Sugiyama, Y., Hagiya, Y., Hayashi, T., Tsuchiya, K., Ishizuka, M., Okura, I., & Ogura, S. (2011). The Effect of 5-Aminolevulinic Acid on Cytochrome c Oxidase Activity. *ALA-Porphyrin Science,* 15–19.

Sugiyama, Y., Hagiya, Y., Nakajima, M., Ishizuka, M., Tanaka, T., & Ogura, S. (2012). The Effect of Aerobic Respiration Activity on Porphyrin Metabolism in Tumor Cells. *Science*, 67–72.

Sugiyama, Y., Hagiya, Y., Nakajima, M., Ishizuka, M., Tanaka, T., & Ogura, S. I. (2014). The heme precursor 5-aminolevulinic acid disrupts the Warburg effect in tumor cells and induces caspase-dependent apoptosis. *Oncology Reports*, 31(3), 1282–1286.

Sun, N., Youle, R. J., & Finkel, T. (2016). The Mitochondrial Basis of Aging. Molecular Cell, 61(5), 654–666.

Takeda, T. A., Sasai, M., Adachi, Y., Ohnishi, K., Fujisawa, J. I., Izawa, S., & Taketani, S. (2017). Potential role of heme metabolism in the inducible expression of heme oxygenase-1. *Biochimica et Biophysica Acta (BBA)-General Subjects*, 1861(7), 1813–1824.

Teodoro, A. J., Oliveira, F. L., Martins, N. B., Maia, G. D. A., Martucci, R. B., & Borojevic, R. (2012). Effect of lycopene on cell viability and cell cycle progression in human cancer cell lines. *Cancer cell international*, 12(1), 1–9.

Trifunovic, A., & Larsson, N. G. (2008). Mitochondrial dysfunction as a cause of ageing. *Journal of Internal Medicine*, 263(2), 167–178.

Wallace, D. C. (1999). Mitochondrial diseases in man and mouse. *Science*, 283(5407), 1482–1488.

Wang, H. E. (2007). Street Drug Toxicity Resulting From Opiates Combined With Anticholinergics. *Prehospital Emergency Care*, *6*(3), 351–354.

Wang, Y. Y., Attané, C., Milhas, D., Dirat, B., Dauvillier, S., Guerard, A., & Muller, C. (2017). Mammary adipocytes stimulate breast cancer invasion through metabolic remodeling of tumor cells. *JCI insight*, 2(4), 1–20.

Willis, J. H., Capaldi, R. A., Huigsloot, M., Rodenburg, R. J. T., Smeitink, J., & Marusich, M. F. (2009). Isolated deficiencies of OXPHOS complexes I and IV are identified accurately and quickly by simple enzyme activity immunocapture assays. *Biochimica et Biophysica Acta - Bioenergetics*, 1787(5), 533–538.

Wilson, M. T., & Brunori, M. (1995). Electron Transfer and Proton Pumping Pathways in Cytochrome. *Biochinie*, 77, 668–676.

Woodard, S. I., & Dailey, H. A. (2000). Multiple regulatory steps in erythroid heme biosynthesis. *Archives of Biochemistry and Biophysics*, *384*(2), 375–378.

Yamashita, N., Watanabe, A., Kondo, H., Kawata, S., Tanaka, T., & Nakajima, M. (2014). Safety test of a supplement, 5-aminolevulinic acid phosphate with sodium ferrous citrate, in diabetic patients treated with oral hypoglycemic agents. *Functional Foods in Health and Disease*, 4(9), 415–428.

Yao, D., Mizuguchi, H., Yamaguchi, M., Yamada, H., Chida, J., Shikata, K., & Kido, H. (2008). Thermal instability of compound variants of carnitine palmitoyltransferase II and impaired mitochondrial fuel utilization in influenza-associated encephalopathy. *Human Mutation*, *29*(5), 718–727.

Yonemura, Y., Endo, Y., Canbay, E., Liu, Y., Ishibashi, H., Mizumoto, A., & Ogura, S. I. (2017). Photodynamic detection of peritoneal metastases using 5-aminolevulinic acid (ALA). *Cancers*, *9*(3), 1–13.

Yoshimoto, M., Higaki, K., Nanba, E., & Ikeguchi, M. (2015). Anti-proliferation activity of fucoidan in MKN45 gastric cancer cells and downregulation of phosphorylated ASK1, a cell cycle-regulated kinase. *Yonago acta medica*, 58(1), 1–7.

Zhang, R., Niu, G., Lu, Q., Huang, X., Chau, J. H., Kwok, R. T., & Tang, B. Z. (2020). Cancer cell discrimination and dynamic viability monitoring through wash-free bioimaging using AIEgens. *Chemical science*, *11*(29), 7676–7684.

CONFERENCE PRESENTATIONS:

1. Arif Suprihadi, Hung Wei Lai, Hui Sin Tan, Motowo Nakajima, Tohru Tanaka, Kiwamu Takahashi, Shun-ichiro Ogura. The effect of heme biosynthesis on the electron transport chain in C2C12 cell line. The 25th Society of Pure and Applied Coordination Chemistry Symposium – Functional complexes leading fusion of multiple scientific fields, November 23–25, 2018 (Okinawa, Japan).
2. Arif Suprihadi, Hung Wei Lai, Hui Sin Tan, Kiwamu Takahashi, Motowo Nakajima, Tohru Tanaka, Shun-ichiro Ogura. The Effect of Heme Biosynthesis on the Mitochondrial Functions in C2C12 cell line. 17th International Photodynamic Association World Congress, June 28–July 4, 2019 (Cambridge, MA, USA)

ACKNOWLEDGMENT

First of all, I thank God for his blessings and guidance. I would like to express the deepest appreciation to my supervisor Assoc. Prof. Dr. Shun-Ichiro Ogura, he continually and convincingly conveyed a spirit of adventure regarding to research and about life in Japan, I am forever grateful to be a part of his laboratory. Very special gratitude goes to the ministry of education, culture, sports, science, and technology (MEXT) Japan for helping and funding, so I can study in Tokyo Institute of Technology without worried about the financial problem. I cannot find words to express my gratitude to my fellow lab mates in Ogura laboratory, thank you to teach me a lot of laboratory stuff and all of the fun we had. I owe a gratitude to all of my friends in Tokyo Institute of Technology especially my fellow Indonesian who coloring my life day by day in Japan. I am also grateful to my eternal cheerleader my family, who provided me through moral and emotional support of my life. And finally, last but by no means least, also to everyone who involves in this journey which I cannot mention one by one.